

Supplemental Methods

Generation of gene targeting mutant mice. Four bacterial artificial chromosome (BAC) clones containing corresponding genomic fragments from B6 or 129 mice (Table S6) were used as templates to make targeting constructs by utilizing Recombineering system (Biological Resourced Branch, National Cancer Institute, Frederick, MD) (1) with a modified Rpsl-kanamycin selection system (2), as previously described (3, 4). First, the BAC clones were transformed into SW102 strain by electroporation. All recombineering procedures were performed in the SW102 transformants. Second, an Rpsl-kanamycin cassette was inserted into corresponding mutation sites by the positive selection with kanamycin. Third, the Rpsl-kanamycin cassette was then replaced with the mutations fragment with 50 bp homologous sequences by the negative selection with streptomycin. Fourth, a LoxP/PGK-Neo/LoxP cassette was inserted into indicated intron sites (Figure S2A) through homology recombination with 76 bp flanking sequences. Fifth, a retrieving plasmid containing a diphtheria toxin (DTA)/5'-arm/AscI/3'-arm cassette or 5'-arm/AscI/3'-arm/DTA cassette was made in a pBluescript SK with an appropriate polylinker. DTA (~1.2kb), 5'-arm (~500bp) and 3'-arm (~500bp) amplified with PCRs using primers flanking appropriate restriction enzyme sites and a DTA template (a gift from Dr. Chingwen Yang, The Rockefeller University, New York, NY) were subcloned into the polyliner sites. Sixth, the designated genomic fragments containing the stop codon mutation and LoxP/PGK-Neo/LoxP cassette were retrieved from the modified BAC clones in SW102 by using AscI-digested retrieving plasmids, as the final targeting vector constructs. All the sequences of the targeting vectors were verified by sequencing with appropriate primers. The linearized targeting vectors from B6 or 129 BAC clones with PacI or NotI were transfected into CY2.4 (B6) or W4 (129) ES cells by electroporation, respectively. Genomic DNA isolated from

G418 and gancyclovir double-resistant ES clones was digested with appropriate restriction enzymes and screened by Southern blot analysis with appropriate probes (Figure S2C). 3 - 13 positives out of 200 G418/gancyclovir-resistant clones were identified except for no positive CY2.4 clones for mE7M vector. Southern blot analysis with additional restriction enzymes and probes further verified single-copy integration of the targeting vector in the correct locus and integrity of the targeting region. After karyotype screening of 3 - 5 positive ES clones, one CY2.4 ES clone (B6) for each of mE3M and mE4M constructs, and two W4 ES clones (129) for each of mE3M, mE4M and mE7M constructs were injected into B6 (W4 ES clones) or B6 albino (CY2.4 ES clones) blastocysts to produce chimeras. There was no germline transmission from mE4M CY2.4 ES clones. Chimeras were bred with B6 or B6 albino to generate F1 mice, which were then bred with CAG-cre/B6 mice to remove the PGK-Neo cassette. The mice from mE3M CY2.4 ES clone were further bred with B6 mice for two generations to produce heterozygous mE3M mice on B6 background (mE3M-B6). The mice from W4 clones were further bred with B6 or 129 for 4 - 5 generations, and followed by 2 - 3-round speed congenic breeding using a Mouse Medium Density Linkage SNP panel containing 1449 loci (Illumina) to produce heterozygous mice with > 99% positive SNPs matching to either B6 or 129 mice. Further breeding these mice with B6 and 129 for 1 - 2 generations produce heterozygous breeders. All WT and homozygous mice generated through heterozygous breeding were determined by genotyping with PCR/restriction enzyme digestion and sequencing (Figures S2D-S2F), and used for all in vivo behavioral and ex vivo studies.

Reverse transcription and quantitative polymerase chain reaction (RT-qPCR). Total RNA isolation of whole brain or the periaqueductal gray (PAG) using miRNeasy Kit (Qiagen) with on-column DNase I treatment and used in RT with Superscript III (Invitrogen) and random

primers, as described previously (5-7). The first-strand cDNAs were used as templates in SYBR green quantitative PCR (qPCR) using HotStart-IT SYBR Green qPCR Master Mix (Affymetrix) and CFX96 Real-Time PCR System (Bio-Rad) to amplify indicated *Oprm1* splice variants, as described previously (6, 7). Three reference genes, succinate dehydrogenase subunit A (SDHA), β_2 -microglobulin (B2M) and glyceraldehyde 3-phosphate dehydrogenase (G3PDH), were used to calculate normalization factors to obtain $2^{-(\Delta Ct)}$ values (6). mE1/2 amplified with primers from exon 1 to exon 2 represented all 7TM C-terminal variants, including the original mMOR-1. All primers and PCR conditions are listed in Table S2.

Opioid receptor binding assays. Whole brain or brain regions including the striatum, nucleus accumbens, thalamus, hypothalamus, periaqueductal gray (PAG) and brainstem were dissected on a mouse Plexiglas brain mold using the atlas of Paxinos and Franklin as described previously (6). Membrane was isolation from mouse whole brain or brain regions or the engineered CHO cells stably transfected with mMOR-1 or mMOR-1C or mMOR-1O construct. [3 H]DAMGO or [3 H]Naloxone or [125 I]Iodobenzoylnaltrexamide (IBNtxA) binding assays were performed at 25°C for 60 min ([3 H]DAMGO or [3 H]Naloxone) or for 90 min ([125 I]IBNtxA) in 50 mM potassium phosphate buffer, pH 7.4, containing 5 mM magnesium sulfate, as described previously (8, 9). Specific binding was defined as the difference between total binding and nonspecific binding, determined in the presence of 10 μ M levallorphan. Protein concentration was determined using a BCA Protein Assay Kit (Pierce). K_d , B_{max} and K_i values were calculated by nonlinear regression analysis (GraphPad Prism 6).

[35 S]GTP γ S binding. 10 – 30 μ g membrane proteins from whole brain or regions were incubated in the presence and absence of various concentrations (0.01 – 30 μ M) of DAMGO or morphine for 60 min at 30°C in the assay buffer (50 mM Tris/HCL, pH 7.7, 3 mM MgCl₂, 0.2

mM EGTA, 10 mM NaCl) containing ~ 0.05 mM [³⁵S]GTPγS and 60 μM GDP, as described previously (10). Basal binding was assessed in the presence of GDP and absence of drug. The incubation was terminated by rapid filtration under vacuum through glass fiber filters, followed by three washes with 3 mL of ice-cold 50 mM Tris-HCl (pH 7.4). Bound radioactivity was determined by liquid scintillation spectrophotometry after overnight extraction in 5 mL of Lquiscint scintillation fluid. EC₅₀ and % maximal stimulation values over basal level were calculated by nonlinear regression analysis (GraphPad Prism 6).

Western blot analysis. Dissected brain regions were homogenized in Tris buffer (50 mM Tris/HCl, 1 mM potassium EDTA and 100 mM NaCl) containing a protease inhibitor mixture containing 2 g/ml each leupeptin, pepstatin, aprotinin, and bestatin and 0.2 mM phenylmethylsulfonyl fluoride. Protein concentration of homogenates was determined using BCA Protein Assay Kit. The homogenates (20 μg/sample) were mixed with SDS sample buffer containing 0.15 M dithiothreitol (DTT) and heated at 100°C for 10 min, separated on a 10% SDS polyacrylamide gel and transferred onto PVDF membranes. The membranes were blocked in a block solution containing TTBS (10 mM Tris/HCl, pH7.4, 150 mM NaCl, and 0.05% Tween 20) and 5% nonfat dried milk at room temperature for 1 h and incubated with a rabbit anti-phospho-ERK1/2 antibody ((1:1,500 dilution, Catalog #: 4370 (D13.14.4E), Cell Signaling)) or a mouse anti-total ERK1/2 antibody ((1:1,000 dilution, Catalog #: 4696 (L34F12), Cell Signaling)) in block solution at 4°C overnight. After washing with TTBS, the membranes were incubated with peroxidase-conjugated mouse anti-rabbit IgG antibody (1:10,000 dilution, Catalog #: 211-032-171, Lot #: 113621, Jackson ImmunoResearch) or goat-anti-mouse IgG antibody (1: 10,000 dilution, Catalog #: 115-035-174. Lot #: 114091, Jackson ImmunoResearch) in TTBS buffer at room temperature for 1 h. After washing with TTBS buffer, signals were developed by using

Luminata Forte Western HRP substrate (Millipore), imaged with ChemiDoc MP (Bio-Rad), and quantified using ImageLab 5.2.

Receptor desensitization study. CHO cells stably expressing mMOR-1, mMOR-1C and mMOR-1O, as previously described(11, 12), were plated on 100 mm dishes, and incubated with 1 μ M DAMGO or morphine for indicated times. Membranes were prepared at each time point and used for [³⁵S]GTP γ S binding assays with 10 μ M DAMGO or morphine.

Locomotor activity. Locomotor activity was measured in 27.3 \times 27.3 cm open-field locomotor activity chambers using open-field activity software (Med Associates). Following injection of morphine (10 mg/kg, i.p.), distance traveled was recorded (in centimeters, (CM)) every minute for 60 min.

Gastrointestinal motility assay. Gastrointestinal transit was determined as described previously (13). After fasting for 24 hours with free access to only water, mice were given an oral gavage of 200 μ l charcoal meal (5% charcoal, 10% gum arabic in water) 10 min after injection of morphine (5 mg/kg, s.c.) or saline. Animals were sacrificed 30 min later, and the distance traveled by charcoal was measured. The percentage of gastrointestinal transit was calculated as follows: % = (Distance traveled by charcoal)/(Total intestine length) \times 100.

Catalepsy. Cataleptic response was assessed by using a horizontal bar test, as described previously ((14, 15). Both front paws of mice were placed on a horizontal bar (3 mm diameter) elevated above the bench with both rear paws in contact with the bench. The time (s) from the placement to removal of the front paws from the bar was recorded as cataleptic response with a maximum cutoff time of 60 s. Following the baseline measurement, mice were administered with saline, or morphine (60 mg/kg, s.c.). Catalepsy was assessed 30 min after morphine administration.

References

1. Lee EC, Yu D, Martinez d, V, Tessarollo L, Swing DA, DL C, Jenkins NA, and Copeland NG. A highly efficient Escherichia coli-based chromosome engineering system adapted for recombinogenic targeting and subcloning of BAC DNA. *Genomics*. 2001;73(1):56-65.
2. Wang S, Zhao Y, Leiby M, and Zhu J. A new positive/negative selection scheme for precise BAC recombineering. *Mol Biotechnol*. 2009;42(1):110-6.
3. Xu J, Lu Z, Xu M, Pan L, Deng Y, Xie X, Liu H, Ding S, Hurd YL, Pasternak GW, et al. A Heroin Addiction Severity-Associated Intronic Single Nucleotide Polymorphism Modulates Alternative Pre-mRNA Splicing of the mu Opioid Receptor Gene OPRM1 via hnRNPH Interactions. *J Neurosci*. 2014;34(33):11048-66.
4. Lu Z, Xu J, Rossi GC, Majumdar S, Pasternak GW, and Pan YX. Mediation of opioid analgesia by a truncated 6-transmembrane GPCR. *J Clin Invest*. 2015;125(7):2626-30.
5. Xu J, Xu M, Brown T, Rossi GC, Hurd YL, Inturrisi CE, Pasternak GW, and Pan YX. Stabilization of the mu-opioid receptor by truncated single transmembrane splice variants through a chaperone-like action. *J Biol Chem*. 2013;288(29):21211-27.
6. Xu J, Lu Z, Xu M, Rossi GC, Kest B, Waxman AR, Pasternak GW, and Pan YX. Differential expressions of the alternatively spliced variant mRNAs of the micro opioid receptor gene, OPRM1, in brain regions of four inbred mouse strains. *PLoS ONE*. 2014;9(10):e111267.
7. Xu J, Faskowitz AJ, Rossi GC, Xu M, Lu Z, Pan YX, and Pasternak GW. Stabilization of morphine tolerance with long-term dosing: Association with selective upregulation of mu-opioid receptor splice variant mRNAs. *Proc Natl Acad Sci U S A*. 2015;112(1):279-84.
8. Pan YX, Xu J, Bolan EA, Abbadie C, Chang A, Zuckerman A, Rossi GC, and Pasternak GW. Identification and characterization of three new alternatively spliced mu opioid receptor isoforms. *MolPharmacol*. 1999;56(396-403).

9. Majumdar S, Grinnell S, Le R, V, Burgman M, Polikar L, Ansonoff M, Pintar J, Pan YX, and Pasternak GW. Truncated G protein-coupled mu opioid receptor MOR-1 splice variants are targets for highly potent opioid analgesics lacking side effects. *Proc Natl Acad Sci U S A*. 2011;108(49):19778-83.
10. Pan L, Xu J, Yu R, Xu MM, Pan YX, and Pasternak GW. Identification and characterization of six new alternatively spliced variants of the human mu opioid receptor gene, Oprm. *Neuroscience*. 2005;133(1):209-20.
11. Pan YX, Xu J, Bolan E, Abbadie C, Chang A, Zuckerman A, Rossi G, and Pasternak GW. Identification and characterization of three new alternatively spliced mu-opioid receptor isoforms. *MolPharmacol*. 1999;56(2):396-403.
12. Xu J, Xu M, Bolan E, Gilbert AK, Pasternak GW, and Pan YX. Isolating and characterizing three alternatively spliced mu opioid receptor variants: mMOR-1A, mMOR-1O, and mMOR-1P. *Synapse*. 2014;68(4):144-52.
13. Paul D, and Pasternak GW. Differential blockade by naloxonazine of two m opiate actions: analgesia and inhibition of gastrointestinal transit. *EurJPharmacol*. 1988;149(403-4).
14. Cheng J, Giguere PM, Schmerberg CM, Pogorelov VM, Rodriguiz RM, Huang XP, Zhu H, McCorvy JD, Wetsel WC, Roth BL, et al. Further Advances in Optimizing (2-Phenylcyclopropyl)methylamines as Novel Serotonin 2C Agonists: Effects on Hyperlocomotion, Prepulse Inhibition, and Cognition Models. *J Med Chem*. 2016;59(2):578-91.
15. Narita M, Takei D, Shiokawa M, Tsurukawa Y, Matsushima Y, Nakamura A, Takagi S, Asato M, Ikegami D, Narita M, et al. Suppression of dopamine-related side effects of morphine by aripiprazole, a dopamine system stabilizer. *Eur J Pharmacol*. 2008;600(1-3):105-9.

Mouse *Oprm1* gene

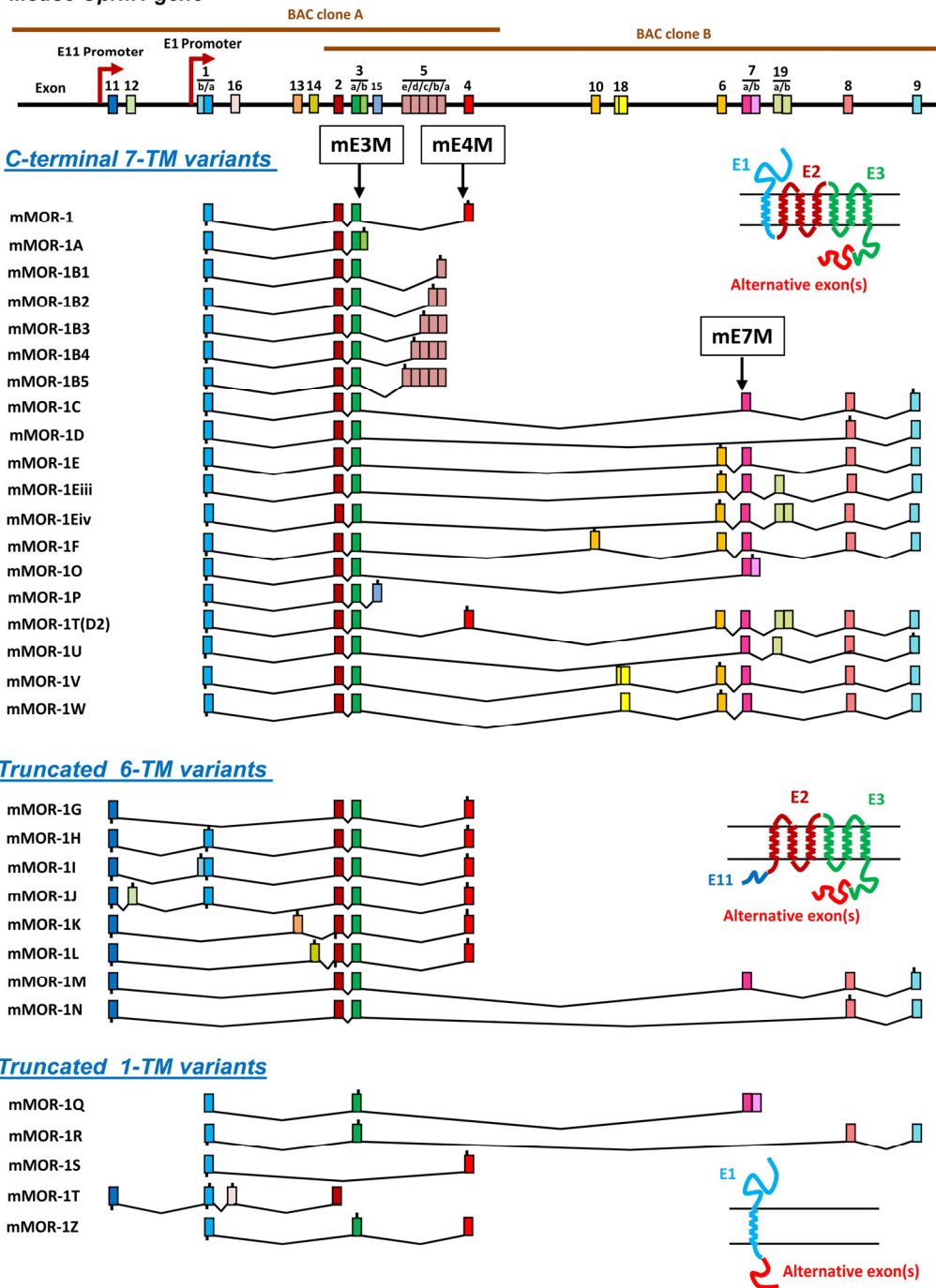


Figure S1. Mouse *Oprm1* gene structure and alternative splicing.

Upper panel: *Oprm1* gene structure. Exons and introns are indicated by color-coded boxes and black horizontal lines, respectively. Two of representative BAC clones used in construction of targeting vectors are indicated by brown lines. Promoters are showed by red arrows. Exons are numbered based upon the published data. **Lower panel:** *Oprm1* alternative splicing. Three classes of alternative splice variants, C-terminal full-length 7-TM variants, truncated 6-TM variants and truncated 1-TM variants, are indicated, and their predicted protein structures shown by cartoon inserts on right, in which color-coded structures match with corresponding color-coded exons (E). For each splice variant, exons are linked by black tilted lines, indicating corresponding splicing. Deduced translation start and stop sites are shown by small lines below and above exon boxes, respectively. mE3M, mE4M and mE7M are the targeted mouse models in which a stop codon was inserted in the end of exon 3 (mE3M), or the beginning of exon 4 (mE4M) or exon 7 (mE7M) (see targeting strategy in Figure S2).

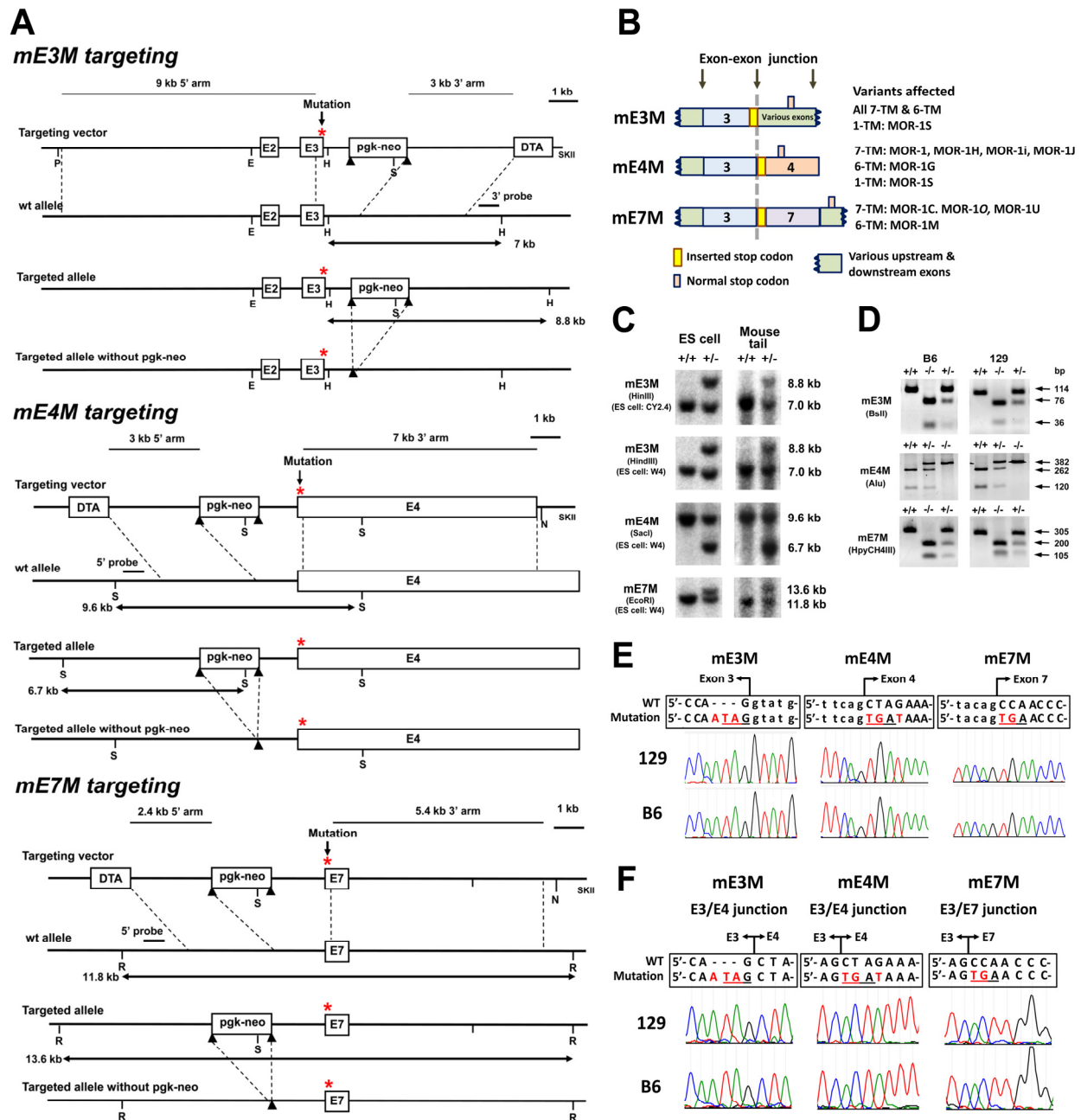


Figure S2. Schematic of gene targeting strategy and characterization of the targeted mouse models. (A). Schematic of gene targeting strategy. Exons (E) and introns are indicated by boxes and horizontal lines. 5' and 3' arms for homologous recombination are shown on the top of targeting vectors. The 3' or 5' probes used in Southern blot and predicted band sizes of WT or targeted allele are indicated. LoxP sites are shown by black triangles. Stop codon mutations are shown by red stars. Restriction enzymes are indicated by single letter. P, PacI; E, EcoRV; H,

HindIII; D, DraI; S, SacI; N, NotI; R, EcoRI. DTA: diphtheria toxin; pgk-neo: phosphoglycerate kinase I promoter-neomycin resistance gene cassette; SKII, pbluescript SKII plasmid.

(B). Schematic of the stop codon insertion on variant mRNAs. Three targeted mouse models, mE3M, mE4M and mE7M, were generated by inserting a stop codon at an appropriate site within indicated exons shown by colored boxes. Inserted and original stop codon are indicated by yellow and pink bars, respectively. In mE3M, a stop codon was inserted at the end of exon 3 to eliminate every C-terminal tails of all 7-TM and 6-TM variants, as well as 1-TM mMOR-1S. In mE4M and mE7M, a stop codon was created at the beginning of exon 4 or exon 7 to eliminate individual C-terminal tails encoded by exon 4 or exon 7 of indicated variants, respectively.

(C). Southern blot analysis. Southern blot analysis was performed as described previously (14,16). Genomic DNAs isolated from ES cells and mouse tails were digested with indicated restriction enzymes, separated on 0.8% agarose gel, and transferred onto GenPlus membrane (NEB). The membranes were hybridized with appropriate [³²P] labeled probes generated by PCR with proper primers (Figure S2B). After washing, the membranes were exposed to Kodak BioMax MS film with MS intensifying screen. Representative data with indicated band sizes are shown. +/+ : WT; +/- : heterozygous.

(D). Genotyping using PCR/restriction enzyme. PCRs were performed using appropriate primers (Table S2), genomic DNAs isolated from mouse tails and platinum Taq DNA polymerase (Invitrogen). The stop codon mutation either creates or eliminates specific recognition sequences of indicated restriction enzymes so that WT, heterozygous and homozygous genotypes can be distinguished by differences in digested band numbers and sizes. The PCR products were then digested with indicated enzymes, separated on 3% MetaPhor agarose (mE3M and mE4M) and 2% regular agarose (mE7M) gels, stained with ethidium bromide and photographed with ChemiDoc MP system (Bio-Rad).

(E). Genomic sequences of mutant alleles in homozygous mice. PCRs were performed using appropriate primers (Table S2) as described in Figure S2D. PCR products were purified by using DNA Clean & Concentrator Kit (Zymo Research), and sequenced with the same sense or antisense primers. Intron and exon sequences are indicated by uppercase and lowercase letters, respectively. Red letters are inserted or mutated sequences. Chromatogram sequences were obtained from sequencing files using dnaTools Xplorer software.

(F). Sequences of RT-PCR products from homozygous mice. Total RNA isolation and RT-PCR were performed using appropriate primers as described in Supplemental Methods (Table S2). The sequences of mE4M and mE7M were obtained using antisense primers and the sequences in the boxes were the complementary sequences.

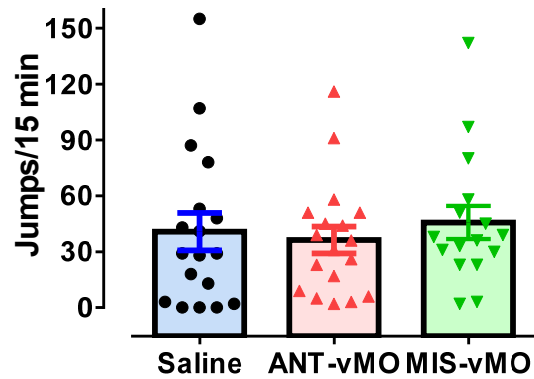


Figure S3. Effect of an antisense vivo-morpholino oligo targeting exon 7 inclusion on morphine physical dependence in CD-1 mice. Group of mice were i.c.v. injected with 10 μ g of an antisense vivo-morpholino oligo (ANT-vMO, n = 18) or a mismatch vivo-morpholino oligo (MIS-vMO, n = 16), or phosphate buffered saline (Saline, n = 18), for four days (Days 1 – 4). Morphine was administered twice-daily (10 mg/kg, s.c.) for 5 days (Days 2 – 6). Morphine dependence was determined on day 6 by measuring jumps within 15 min immediately following naloxone injection (s.c., 30 mg/kg) 3 hours after the last morphine treatment. Results are mean \pm SEM from two independent experiments. 1-way ANOVA showed no significant differences among the groups.

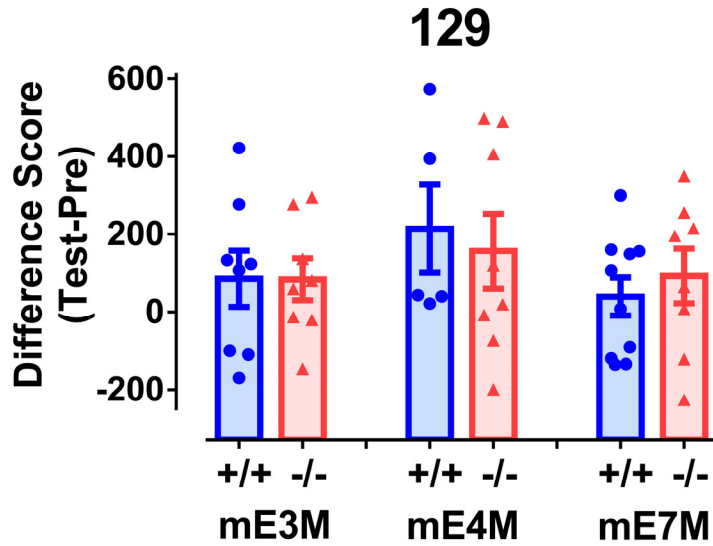


Figure S4. Effect of the C-terminal truncation on morphine conditioned place preference (CPP) in the mutant mice on 129 background. Morphine CPP was assessed using a three-chamber apparatus (Med Associates) with a 6-day paradigm as described in Methods. Results were calculated by different scores (sec) in drug-paired chamber between the test day and preconditioning day. The number of mice used were: mE3M-129, WT (+/+) & homozygous (-/-): 8; mE4M-129, +/+ : 5 & -/-: 8; mE7M-29, +/+ : 10 & -/-: 8. 1-way ANOVA showed that there were no significant differences among groups.

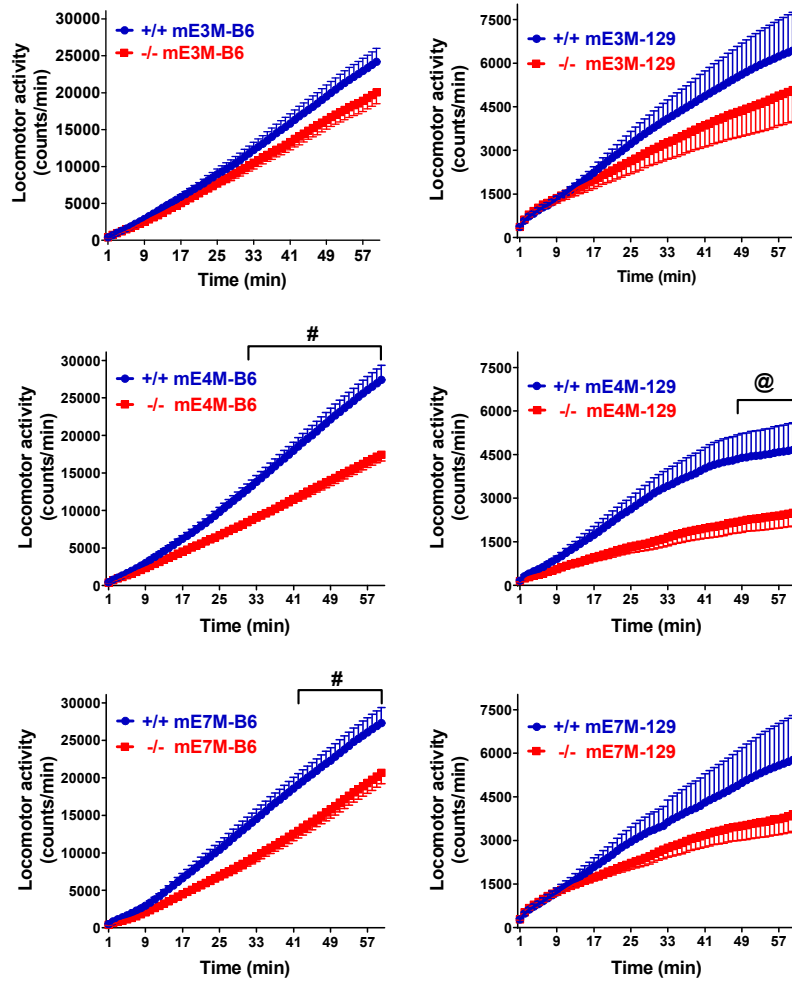


Figure S5. Effect of the C-terminal truncation on morphine locomotor activity in the mutant mouse models. Locomotor activity was measured in 27.3×27.3 cm open-field locomotor activity chambers using open-field activity software (Med Associates). Following injection of morphine (10 mg/kg, i.p.), locomotor activity was measured at 1 min intervals for 60 min. The number of mice used were same as described in Fig. 3A. #: compared to +/+, $p < 0.05 - 0.001$; @: compared to +/+, $p < 0.05$ (2-way ANOVA with Bonferroni's *post hoc* test).

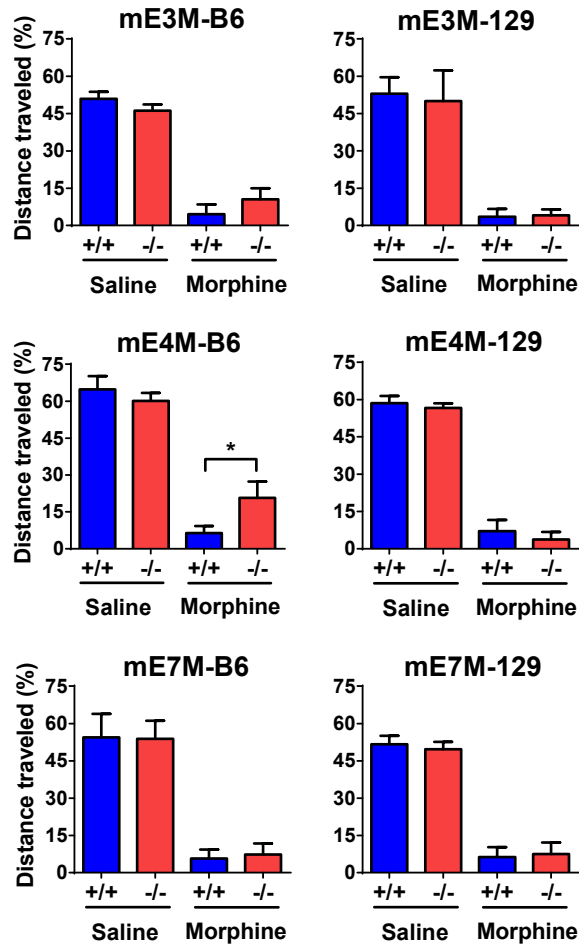


Figure S6. Effect of the C-terminal truncation on morphine inhibition of gastrointestinal (GI) transit in the mutant mouse models. Morphine induced inhibition of GI transit was measured as described in Supplemental Methods. The percentage (%) of distance traveled was calculated as follows: % = (Distance traveled by charcoal)/(Total intestine length) x 100. Results are the mean \pm SEM from group of mice (n = 5 – 7) except for mE4M-B6 (n = 10 – 16 in two independent experiments). Compared to +/+ treated with morphine, *: $p < 0.05$ (1-way ANOVA with Bonferroni's *post hoc* test).

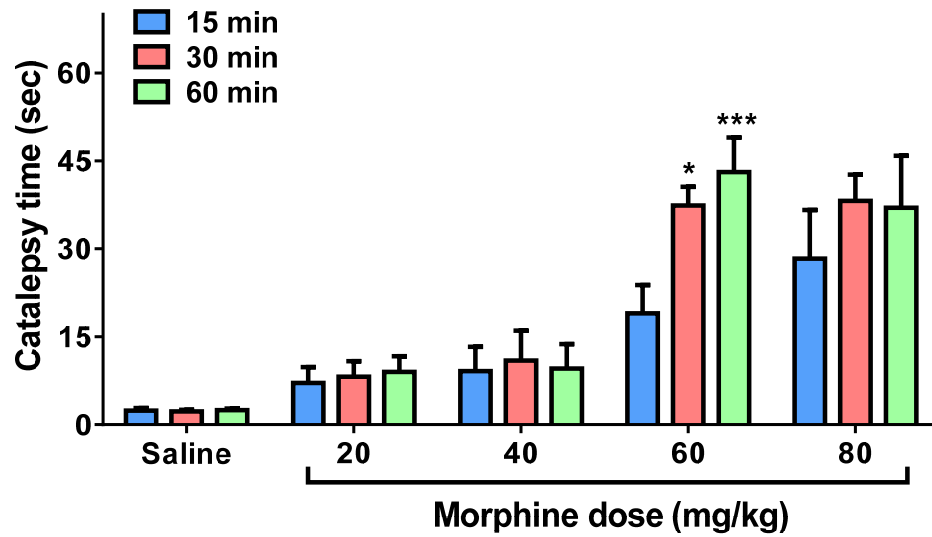


Figure S7. Morphine-induced catalepsy. Cataleptic response was assessed by using a horizontal bar test, as described in Supplemental Methods. Groups of B6 mice ($n = 3-8$) were s.c. injected with indicated doses of morphine or saline. Catalepsy was measured at indicated times after morphine administration. Compared to 15 min, *: $p < 0.05$; ***: $p < 0.001$ (2-way ANOVA with Bonferroni's *post hoc* test).

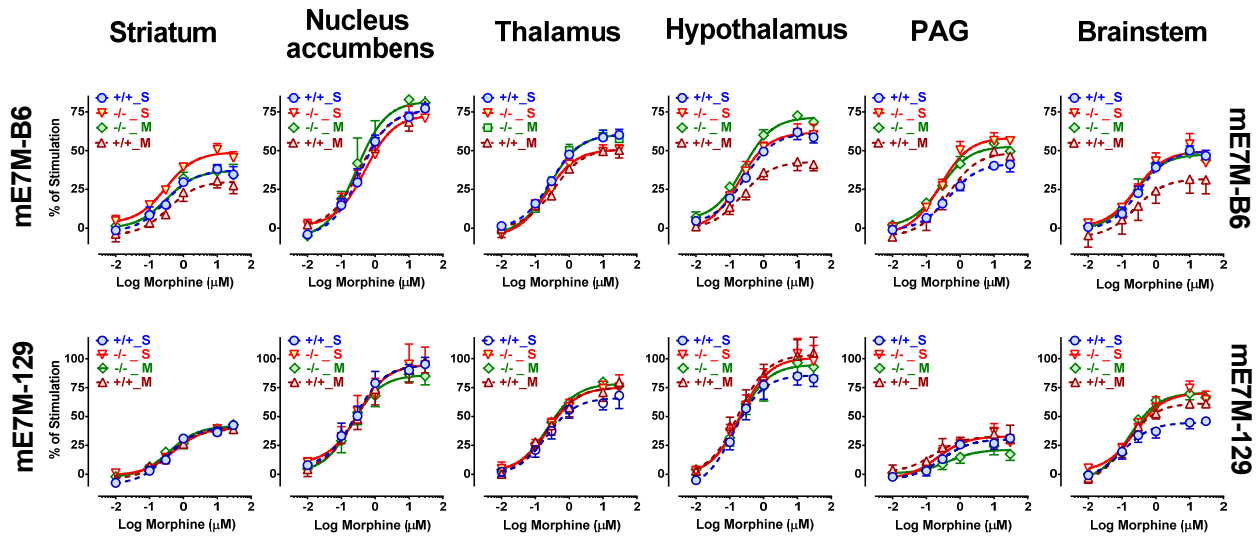


Figure S8. Effect of the truncation of exon 7-encoded C-terminal tails on morphine-induced receptor desensitization by [³⁵S]GTP γ S binding assay in six brain regions of mE7M-B6 and mE7M-129 mice. mE7M-B6 and mE7M-129 WT (+/+) and homozygous (-/-) mice were treated with morphine (M) in the same way as in morphine tolerance studies (Figure 1). A control group injected with saline (S) was also included for both WT and homozygous mice. Membranes from six brain regions dissected on day 5 after the last morphine injection were used in [³⁵S]GTP γ S binding assay, as described in Supplemental Methods, % maximal stimulation (over basal level) and EC₅₀ values were calculated by nonlinear regression analysis (Prism). Each dose-response curve was from three to four independent experiments. All the EC₅₀ and % maximal stimulation values and the results from statistical analysis using 2-way ANOVA are listed in Table 5.

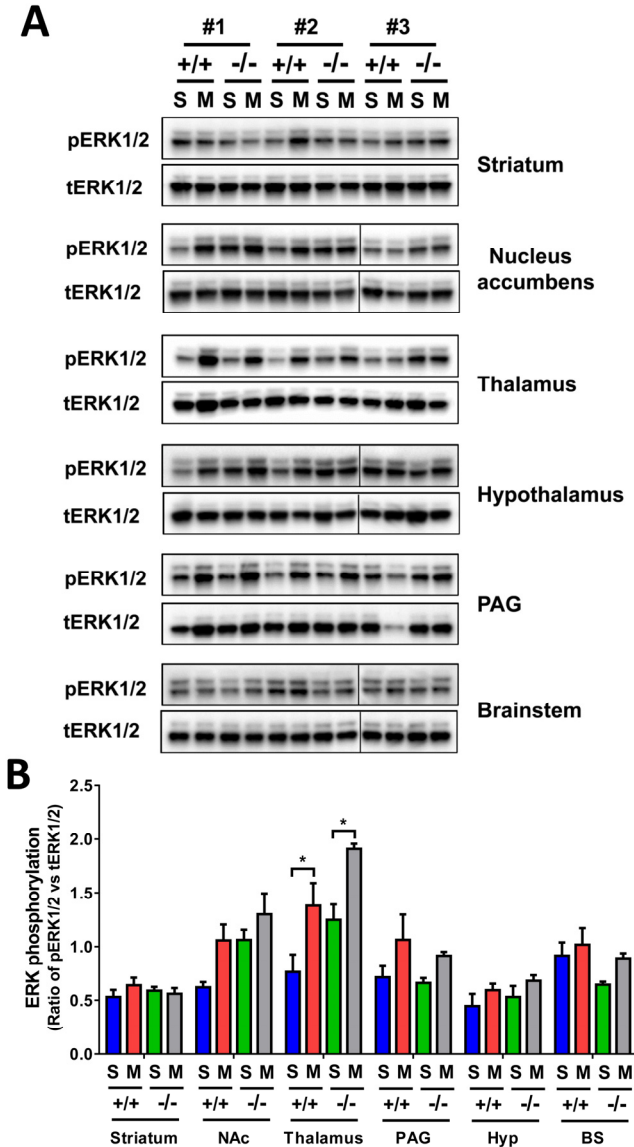


Figure S9. Effect of the truncation of exon7-encoded C-terminal tails on morphine-induced ERK1/2 activation in six brain regions of mE7M-B6 mice. (A) Western blot. mE7M-B6 WT (+/+) and homozygous (-/-) mice were treated with morphine (M) in the same way as in morphine tolerance studies (Figures 1). A control group injected with saline (S) was also included for both WT and homozygous mice. Whole cell lysate from six brain regions dissected on day 5 after the last morphine injection were used in Western blot with an anti-phospho-ERK1/2 (for pERK1/2) and an anti-total ERK1/2 antibody (for tERK1/2), as described in Supplemental Methods. Three independent samples (#1, #2 and #3) were used. All the samples from each region were run on the same gel. The #3 samples in the nucleus accumbens, hypothalamus and brainstem were re-arranged from the same blot, as indicated by a separated line, to keep the samples in the same order. (B) Quantification of Western blot. Band intensities on the images obtained in ChemiDoc MP (Bio-Rad) were quantified using ImageLab 5.2. Results are the ratios of pERK1/2 and tERK1/2. *: compared to Saline control, $p < 0.01$ (2-way ANOVA with Bonferroni's *post hoc* test).

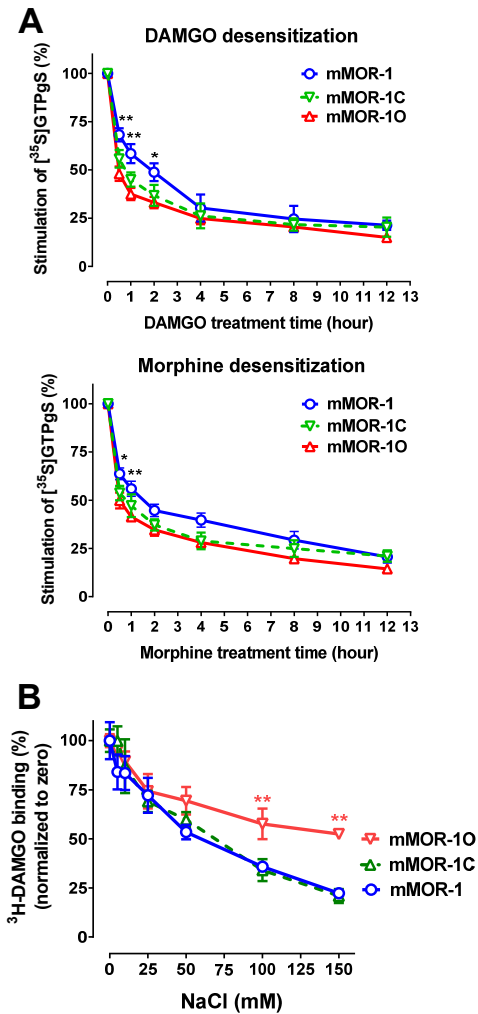


Figure S10. In vitro characterization of C-terminal 7-TM variants in CHO cells. (A) DAMGO- and morphine-induced receptor desensitization. Membrane was isolated from CHO cells stably transfected with E4-associated mMOR-1 and E7-associated mMOR-1C and mMOR-1O treated with 1 μ M DAMGO or morphine for indicated times, and used in [³⁵S]GTP γ S binding assay with 10 μ M DAMGO or morphine, as described in Supplemental Methods. The % Stimulation over basal level was normalized with 0 time point. Results are the mean \pm SEM from at least three independent determinations. Compared to mMOR-1O, *: $p < 0.05$; **: $p < 0.01$ (2-way ANOVA with Bonferroni's *post hoc* test). **(B)** Effect of sodium on [³H]DAMGO binding. Membrane from the same CHO cells as (A) was used in [³H]DAMGO (\sim 1nM) binding containing indicated concentrations of sodium chloride (NaCl). Specific binding, determined by the difference between total binding and nonspecific binding in the presence of 10 μ M levallorphan, was normalized with that at 0 mM NaCl. Compared to mMOR-1C or mMOR-1O, $p < 0.01$ (2-way ANOVA with Bonferroni's *post hoc* test).

Exon 7 Exon 8

```

mouse -P1TLAV2SVAQIF3TY4PS5PTHVEKPKCK6SCMDRGMRNLLPDDGPRQ8ESGEGQLGR*
rat   -PALAVSVAQIF3TY4PS5PTHGEKPKCK7SYRDR-
human -PPLAVSMAQIF3TRY4SP5PTHREK9TCNDY10MKR*
(exon O)@

```

		Predicted protein kinase
1	T	PKC/CAMK/CK1/PLK
2	S	PKC/CAMK/CK1/CMGC
3	T	GRK/PKC/CK1/CMGC
4	Y	MET/Src/Tec
5	S	GRK/CMGC/CK1/
6	T	GRK/CAMK/CK1/CMGC
7	S	GRK/PKC/CAMK/CK1
8	S	PKC/CAMK/MAPK/CK1
9	T	GRK/CAMK/CK1/CMGC
10	Y	MET/Src/Tec/Jak

Figure S11. Alignment of deduced amino acid sequences from exon 7-associated C-terminal tails among mouse, rat and human and their predicted phosphorylation sites and protein kinases. Deduced amino acid sequences from mouse, rat and human were aligned using VectorNTI software (Invitrogen). Human exon O is a homologue of mouse or rat exon 7. Potential phosphorylation sites and corresponding protein kinases were predicted using a GPS webserver (67). The underlined sequences represent a consensus β -arrestin binding motif, PxPxxE or PxxPxxE, proposed based on homology modeling with the recent crystal structure of rhodopsin-arrestin complex as a template (68) (H.E. Xu, personal communication). [@]: #5 serine residue in human exon O is predicted from a single nucleotide polymorphism (rs75433176) as a T, while the original C predicts a proline. Red letters: predicted phosphorylated sites as serine (S) or threonine (T) residues; Green letters: predicted phosphorylated sites as tyrosine residue; *: stop codon; PKC: protein kinase C; CAMK: Ca²⁺/calmodulin-dependent protein kinase; CK1: casein kinase 1; PLK: polo-like kinase; CMGC: a family protein kinases including cyclin-dependent kinases, mitogen-activated protein kinases, glycogen synthase kinases and CDK-like kinases; GRK: G protein-coupled receptor kinase; MET: Met receptor tyrosine kinase; Src: Src protein-tyrosine kinase; Tec: TEC-family protein tyrosine kinases; MAPK: mitogen-activated protein kinase; Jak: Janus kinase.

Table S1. Expressions of *Oprm1* splice variant mRNAs in the targeted mouse models by RT-qPCR

Variant	mE3M-129		mE3M-B6		mE4M-129		mE4M-B6		mE7M-129		mE7M-B6	
	+/+	-/-	+/+	-/-	+/+	-/-	+/+	-/-	+/+	-/-	+/+	-/-
7-TM variants												
mE1-2 ^A	100 ± 5 ^B	90 ± 1	100 ± 8	98 ± 8	100 ± 2	100 ± 9	100 ± 2	88 ± 4	100 ± 2	98 ± 9	100 ± 4	94 ± 5
mMOR-1A	100 ± 8	92 ± 21	100 ± 7	100±23	100 ± 4	75 ± 8	100±23	69 ± 11	100 ± 4	105 ± 6	100 ± 1	116±22
mMOR-1C	100 ± 3	15 ± 4*	100±22	15 ± 7*	100 ± 1	86 ± 8	100±11	102 ± 5	100±13	20 ± 7 [#]	100 ± 9	12 ± 1*
mMOR-1D	100 ± 7	88 ± 11	100±32	96 ± 43	100±14	77 ± 14	100 ± 6	83 ± 24	100 ± 3	85 ± 20	100 ± 2	97 ± 12
mMOR-1i	100 ±10	104 ± 5	100±11	94 ± 3	100 ± 8	88 ± 10	100±15	99 ± 6	100 ±18	97 ± 10	100 ±11	96 ± 10
mMOR-1O	100 ±12	86 ± 9	100±26	97 ± 10	100 ± 5	96 ± 17	100±20	88 ± 9	100 ±16	124 ±17	100 ±15	89 ± 14
6-TM variants												
mMOR-1G	100±29	105±41	100±11	98 ± 23	100±28	96 ± 6	100 ± 7	83 ± 19	100±10	95 ± 32	100±21	94 ± 19
mMOR-1M	100±21	9 ± 8 [@]	100 ± 6	4 ± 2 [@]	100±25	93 ± 35	100±17	98 ± 27	100±32	6 ± 3 [@]	100 ± 9	5 ± 2 [@]
mMOR-1K	100 ± 3	116 ±11	100 ± 6	88 ± 18	100 ± 1	112±12	100 ± 5	94 ± 28	100 ±11	107±14	100 ±10	100 ± 2
1-TM variants												
mMOR-1S	100±16	122±16	100±17	97 ± 2	100 ± 1	66 ± 11	100 ± 8	40 ± 8	100 ± 9	95 ± 19	100 ± 5	117±48
mMOR-1R	100 ± 1	98 ± 18	100 ± 8	92 ± 10	100 ± 6	106±14	100 ± 1	96 ± 3	100±12	85 ± 12	100 ± 8	98 ± 7

^A: mE1-2 amplified with primers from exon 1 to exon 2 represented all C-terminal variants, including the original mMOR-1.

^B: All 2^{-(ΔCt)} values are normalized with WT (+/+) so all the values of WT are defined as 100%. Results are the mean ± SEM of at least three independent determinations. Compared to +/+: *: $p < 0.0001$; #: $p < 0.001$; @: $p < 0.01$ (1-way ANOVA with Bonferroni's *post hoc* test).

Table S2. List of primers and PCR conditions.

Variant	Sense Primer (SP)			Antisense Primer (AP)		
	Name of SP	Sequences of SP	Location of SP	Name of AP	Sequences of AP	Location of AP
Primers used in qPCRs (Table 1 and Fig. 2.)						
mE1-2	SP-1	GCAGAGGAGAATATCGGACGCTCAG	E1	AP-1	GTCTTCATTTTGGTATATCTTACAATCACATACATG	E1/2 joint
mE3-4	SP-2	CAAATAACAGGCAGGGGTCCATAGATTG	E2/3 joint	AP-2	CCAGATTTTCTAGCTGGTGGTTAGTTC	E3/4 joint
mE3-7	SP-2	CAAATAACAGGCAGGGGTCCATAGATTG	E2/3 joint	AP-3	CAGGGTTGGCTGGTGGTTAGTTC	E3/7 joint
mMOR-1A	SP-3	CACAAAATACAGGCAGGGGTCCA	E2/3 joint	AP-4	CTAAATCTTAGACTGGTATCAGGTGCTGTG	E3a
mMOR-1C	SP-4	GCACTGATCACGATTCCAGAAACCAC	E1	AP-5	CAGGGTTGGCTGGTGGTTAGTTC	E3/7 joint
mMOR-1D	SP-4	GCACTGATCACGATTCCAGAAACCAC	E1	AP-6	GGTTCCTCATTCTCTGGTGGTTAGTTC	E3/8 joint
mMOR-1i	SP-5	GGAAGAGTTACCTCAGCCTCTGGATCC	E11/1b joint	AP-1	GTCTTCATTTTGGTATATCTTACAATCACATACATG	E1/2 joint
mMOR-1O	SP-6	GAACTAACCACCAGCCAACCCTG	E3/7 joint	AP-7	CTAATCCTCGCCGTGCAAAAAGCTAAAC	E7a
mMOR-1G	SP-7	GGAAGAGTTACCTCAGATATACAAAATGA	E11/2 joint	AP-8	CCAGATTTTCTAGCTGGTGGTTAGTTC	E3/4 joint
mMOR-1M	SP-7	GGAAGAGTTACCTCAGATATACAAAATGA	E11/2 joint	AP-9	CAGGGTTGGCTGGTGGTTAGTTC	E3/7 joint
mMOR-1K	SP-8	GTCGACCACCACAAAGATATACAAAATG	E14/2 joint	AP-10	GCCACGTTCCCATCAGGTAGTTAACAC	E2
mMOR-1S	SP-9	GGCTCCTGGCTCAACTTGTCAC	E1	AP-11	CCAGATTTTCTAGCTAGTGGAAACCAGAG	E1/4 joint
mMOR-1R	SP-10	ATGTATGTGATTGTAAGGGTCCATAGATTG	E1/3 joint	AP-12	GGTTCCTCATTCTCTGGTGGTTAGTTC	E3/8 joint
mSDHA	SP-11	TGCCTCTGTGGTTGAGCTAGAA		AP-13	TCATATCGCAGAGATCTTCATACAACG	
mB2M	SP-12	ATTCACCCCCACTGAGACTG		AP-14	TGCTATTTCTTTCTGCGTGC	
G3PDH	SP-13	ACCACAGTCCATGCCATCAC		AP-15	TCCACCACCCTGTTGCTGTA	

Melting curve was performed after the cycling;

Primers used in regular PCR for genotyping and sequencing (Fig. S2.)

mE3M_gDNA	SP-14	CCTCCACGGCTAATACAGTGGATCG		AP-16	CTTAAGGATCTAAATCTTAGACTGGTATCAGGTGC	
mE4M_gDNA	SP-15	CAATGTTCCAGGGACTGCAAG		AP-17	GGATGTTTCTGTACATGAGCTGGATTC	
mE7M_gDNA	SP-16	CCAACCTCGCAGAGAATCCCTTCC		AP-18	GCATGAATGAAAACGTCTAATCCTCG	
mE3M_mRNA	SP-17	GCCTGAACCCAGTTCTTTATGCG		AP-19	GCAACCTGATTCCAAGTAGATGGCAGC	
mE4M_mRNA	SP-17	GCCTGAACCCAGTTCTTTATGCG		AP-19	GCAACCTGATTCCAAGTAGATGGCAGC	
mE7M_mRNA	SP-17	GCCTGAACCCAGTTCTTTATGCG		AP-20	CTAATCCTCGCCGTGCAAAAAGCTAAAC	

SP: sense primer; AP: antisense primer; SDHA: succinate dehydrogenase subunit A; B2M: β 2-microglobulin; G3PDH: glyceraldehyde 3-phosphate dehydrogenase; gDNA: genomic DNA.

Variant	Initial	Cycling (35-45)		
	Denaturing	Denaturing	Annealing	amplification

mE1-2	95°C, 2 min	95°C, 15 sec	65°C, 30 sec	72°C, 30 sec
mE3-4	95°C, 2 min	95°C, 15 sec	65°C, 30 sec	72°C, 30 sec
mE3-7	95°C, 2 min	95°C, 15 sec	65°C, 30 sec	72°C, 30 sec
mMOR-1A	95°C, 2 min	95°C, 15 sec	65°C, 30 sec	72°C, 40 sec
mMOR-1C	95°C, 2 min	95°C, 15 sec	65°C, 30 sec	72°C, 40 sec
mMOR-1D	95°C, 2 min	95°C, 15 sec	65°C, 30 sec	72°C, 40 sec
mMOR-1i	95°C, 2 min	95°C, 15 sec	65°C, 30 sec	72°C, 30 sec
mMOR-1O	95°C, 2 min	95°C, 15 sec	63°C, 30 sec	72°C, 30 sec
mMOR-1G	95°C, 2 min	95°C, 15 sec	59°C, 30 sec	72°C, 60 sec
mMOR-1M	95°C, 2 min	95°C, 15 sec	60°C, 30 sec	72°C, 60 sec
mMOR-1K	95°C, 2 min	95°C, 15 sec	65°C, 30 sec	72°C, 30 sec
mMOR-1S	95°C, 2 min	95°C, 15 sec	65°C, 30 sec	72°C, 30 sec
mMOR-1R	95°C, 2 min	95°C, 15 sec	62°C, 30 sec	72°C, 60 sec
mSDHA	95°C, 2 min	95°C, 15 sec	60°C, 30 sec	72°C, 60 sec
mB2M	95°C, 2 min	95°C, 15 sec	60°C, 30 sec	72°C, 60 sec
G3PDH	95°C, 2 min	95°C, 15 sec	60°C, 30 sec	72°C, 60 sec

Melting curve was performed after the cycling;

Primers used in regular PCR for genotyping and sequencing (Fig. S2.)

mE3M_gDNA	94°C, 2 min	94°C, 15 sec	65°C, 20 sec	72°C, 30 sec
mE4M_gDNA	94°C, 2 min	94°C, 15 sec	65°C, 20 sec	72°C, 30 sec
mE7M_gDNA	94°C, 2 min	94°C, 15 sec	65°C, 20 sec	72°C, 30 sec
mE3M_mRNA	94°C, 2 min	94°C, 15 sec	65°C, 20 sec	72°C, 30 sec
mE4M_mRNA	94°C, 2 min	94°C, 15 sec	65°C, 20 sec	72°C, 30 sec
mE7M_mRNA	94°C, 2 min	94°C, 15 sec	65°C, 20 sec	72°C, 30 sec

Table S3. Competition studies using [³H] DAMGO in the targeted mouse models

Mouse model	Genotype	K_i (nM) ^A				
		<i>Morphine</i>	<i>M6G</i>	<i>Naloxone</i>	<i>Dynorphin A</i>	<i>B-endorphin</i>
mE3M-129	+/+	0.9 ± 0.2 ^B	3.5 ± 1.8	0.8 ± 0.2	13 ± 6	4.1 ± 0.6
	-/-	0.2 ± 0.0	1.2 ± 0.5	0.4 ± 0.1	3.4 ± 1.8	1.5 ± 0.2
mE3M-B6	+/+	0.6 ± 0.1	1.6 ± 0.9	0.9 ± 0.3	11 ± 7	3.4 ± 0.7
	-/-	0.4 ± 0.1	0.6 ± 0.3	0.5 ± 0.1	5.8 ± 2.8	1.8 ± 0.2
mE4M-129	+/+	0.6 ± 0.1	3.5 ± 0.6	0.9 ± 0.4	10 ± 5	3.8 ± 1.3
	-/-	0.4 ± 0.2	2.1 ± 0.4	0.8 ± 0.3	5.8 ± 2.2	2.7 ± 0.5
mE4M-B6	+/+	0.8 ± 0.2	2.8 ± 0.6	0.9 ± 0.1	13 ± 5	3.5 ± 1.3
	-/-	0.3 ± 0.1	2.7 ± 0.0	0.8 ± 0.1	7.7 ± 0.4	4.8 ± 1.5
mE7M-129	+/+	1.0 ± 0.3	4.3 ± 2.8	0.5 ± 0.1	14 ± 6	3.9 ± 1.5
	-/-	1.1 ± 0.1	1.3 ± 0.2	0.8 ± 0.2	7.4 ± 0.7	2.0 ± 0.1
mE7M-B6	+/+	1.0 ± 0.4	4.4 ± 1.2	1.4 ± 0.8	11 ± 4	2.4 ± 0.4
	-/-	0.5 ± 0.1	2.7 ± 1.3	0.7 ± 0.4	4.8 ± 1.8	1.5 ± 0.2

^A: Competition studies against [³H]DAMGO (approximately 1 nM) were performed with indicated ligands and the K_i value calculated as described in Supplemental Methods. ^B: Results are the means \pm SEM of at least three independent determinations. 1-way ANOVA with Bonferroni's *post hoc* test showed no significant difference between WT (+/+) and homozygous (-/-) mice.

Table S4. Saturation studies using [³H]DAMGO binding

Region	Mouse	mE7M-B6		mE7M-129	
		K_d (nM) ^A	B_{max} (fmol/mg protein) ^A	K_d (nM)	B_{max} (fmol/mg protein)
Hypothalamus	+/+ _{-S}	0.57 ± 0.2	46 ± 3	0.34 ± 0.0	65 ± 1
	+/+ _{-M}	0.37 ± 0.1	43 ± 5	0.42 ± 0.1	62 ± 6
	-/- _{-S}	0.36 ± 0.1	47 ± 3	0.33 ± 0.0	64 ± 3
	-/- _{-M}	0.38 ± 0.1	47 ± 8	0.38 ± 0.1	58 ± 2
Brainstem	+/+ _{-S}	0.42 ± 0.0	31 ± 2	0.25 ± 0.0	43 ± 4
	+/+ _{-M}	0.48 ± 0.1	30 ± 5	0.41 ± 0.1	43 ± 3
	-/- _{-S}	0.42 ± 0.1	33 ± 4	0.35 ± 0.1	37 ± 4
	-/- _{-M}	0.63 ± 0.1	37 ± 3	0.41 ± 0.1	42 ± 4

^A: [³H]DAMGO saturation studies were performed in membranes prepared from the hypothalamus and brainstem of indicated mouse models as described in Supplemental Methods. The KD and B_{max} values were determined by nonlinear regression analysis (Prism). Results are the mean ± SEM of at least three independent saturation studies. 1-Way ANOVA revealed no significant differences among groups in the Kd and B_{max} values. +/+_{-S}, +/+_{-M}, -/-_{-S} and -/-_{-M}: WT (+/+) or homozygous (-/-) mice treated with saline (S) or morphine (M), respectively.

Table S5. Mu agonist-induced β -arrestin2 recruitment and G protein activation of mMOR-1, mMOR-1C and mMOR-1O in an engineered CHO cell line.

Variants	Ligands	β -arrestin 2 recruitment		G protein activation	
		E _{max} (%)	EC ₅₀ (nM)	E _{max} (%)	EC ₅₀ (nM)
mMOR-1	DAMGO	102 ± 2	112 ± 19	101 ± 4	17 ± 6
	Morphine	16 ± 1	156 ± 20	115 ± 7	25 ± 7
	Endomorphin1	63 ± 5	121 ± 25	97 ± 7	44 ± 8
	Fentanyl	65 ± 16	40 ± 5	93 ± 12	22 ± 1
mMOR-1C	DAMGO	94 ± 3	355 ± 94*	99 ± 2	195 ± 77*
	Morphine	17 ± 1	195 ± 16	92 ± 4*	53 ± 18
	Endomorphin1	72 ± 2	214 ± 26*	91 ± 2	116 ± 28
	Fentanyl	49 ± 2	48 ± 5	89 ± 5	59 ± 10
mMOR-1O	DAMGO	101 ± 4	120 ± 6 [@]	99 ± 1	157 ± 6
	Morphine	31 ± 6 ^{*,@}	162 ± 21	64 ± 1 ^{***,@@}	123 ± 24 ^{***,@}
	Endomorphin1	79 ± 3*	109 ± 20 [@]	83 ± 2	282 ± 73 ^{***,@}
	Fentanyl	83 ± 2 [@]	31 ± 5 [@]	110 ± 3	163 ± 24

β -arrestin2 recruitment and [³⁵S]GTP γ S binding assays were performed in an engineered CHO cell line stably expressing the mMOR-1 or, mMOR-1C or mMOR-1O construct in ProLink vector, as described in Supplemental Methods. Saturation studies using [¹²⁵I]IBNtxA binding showed the B_{max} values (5.79±0.32, 4.18±0.14 and 1.07±0.17 pmol/mg protein for mMOR-1, mMOR-1C and mMOR-1O, respectively), and K_D values (0.10±0.01, 0.19±0.01 and 0.24±0.06 nM, for mMOR-1, mMOR-1C and mMOR-1O, respectively). The data was normalized to maximal DAMGO stimulation (10 μ M). The E_{max} and EC₅₀ values were determined by nonlinear regression analysis (Prism). Results are the mean ± SEM of three independent experiments (n = 3). Compared to mMOR-1: *: $p < 0.05$; **: $p < 0.01$; ***: $p < 0.001$. Compared to mMOR-1C: @: $p < 0.05$.; @@: $p < 0.01$ (1-way ANOVA with Bonferroni's *post hoc* test).

Table S6. BAC clones used in construction of targeting vectors

Clone ID	Mouse strain	Source	Targeting vector	ES cell injected	Mouse model
RP24-288N13	B6	BACPAC Resource Center	mE3M	CY2.4	mE3M-B6
			mE4M	CY2.4	---
RP24-164E12	B6	BACPAC Resource Center	mE7M	---	---
BACM-350522	129	Genome Systems Inc	mE3M	W4	mE3M-129
			mE4M	W4	mE4M-129 mE4M-B6
RP24-525N22	129	BACPAC Resource Center	mE7M	W4	mE7M-129 mE7M-B6

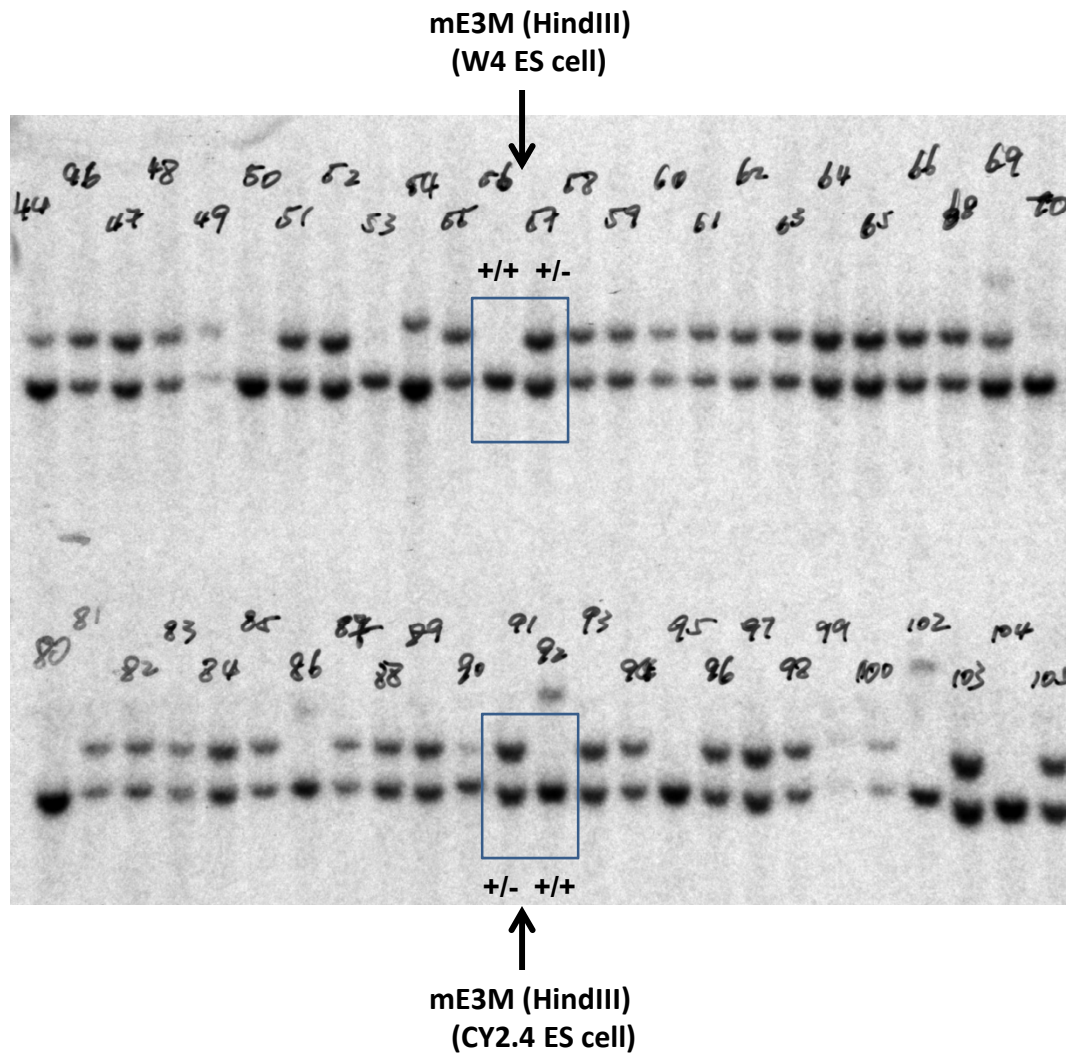


Figure S2C. mE3M (HindIII) ES cell: W4 and ES cell: CY2.4.

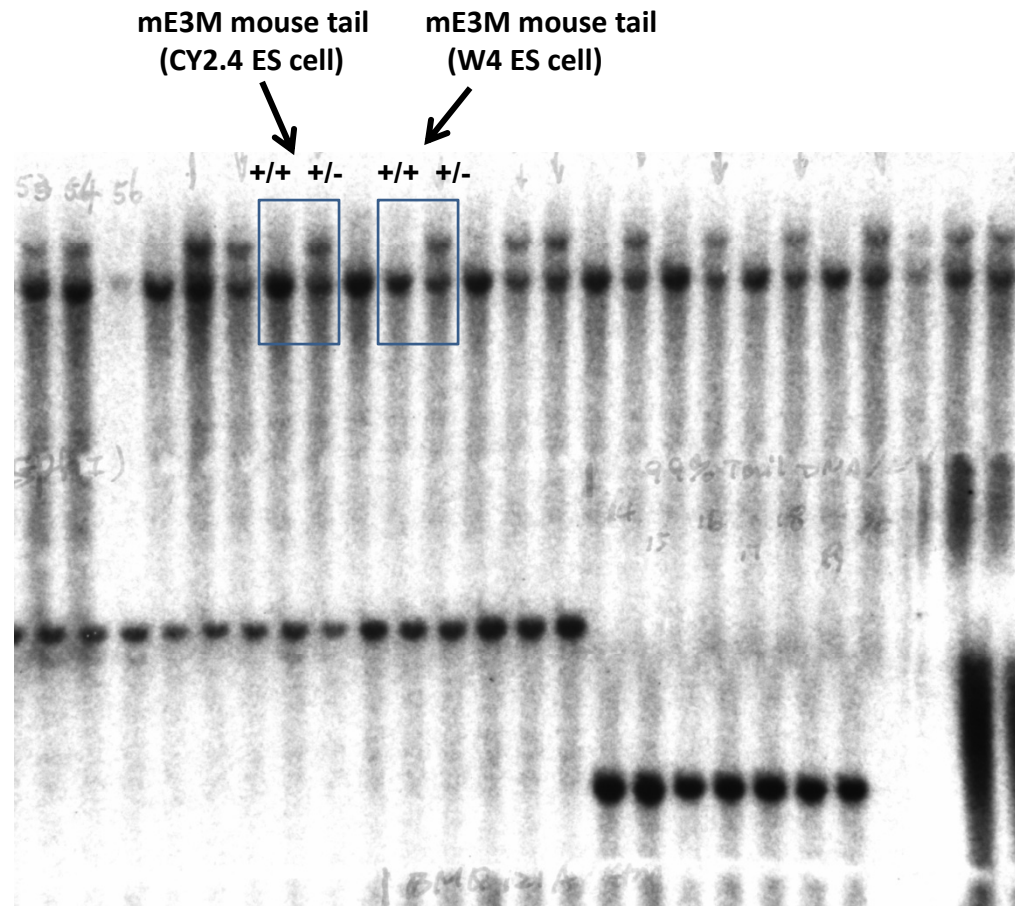


Figure S2C. mE3M (HindIII) mouse tail (W4) and mouse tail (CY2.4).

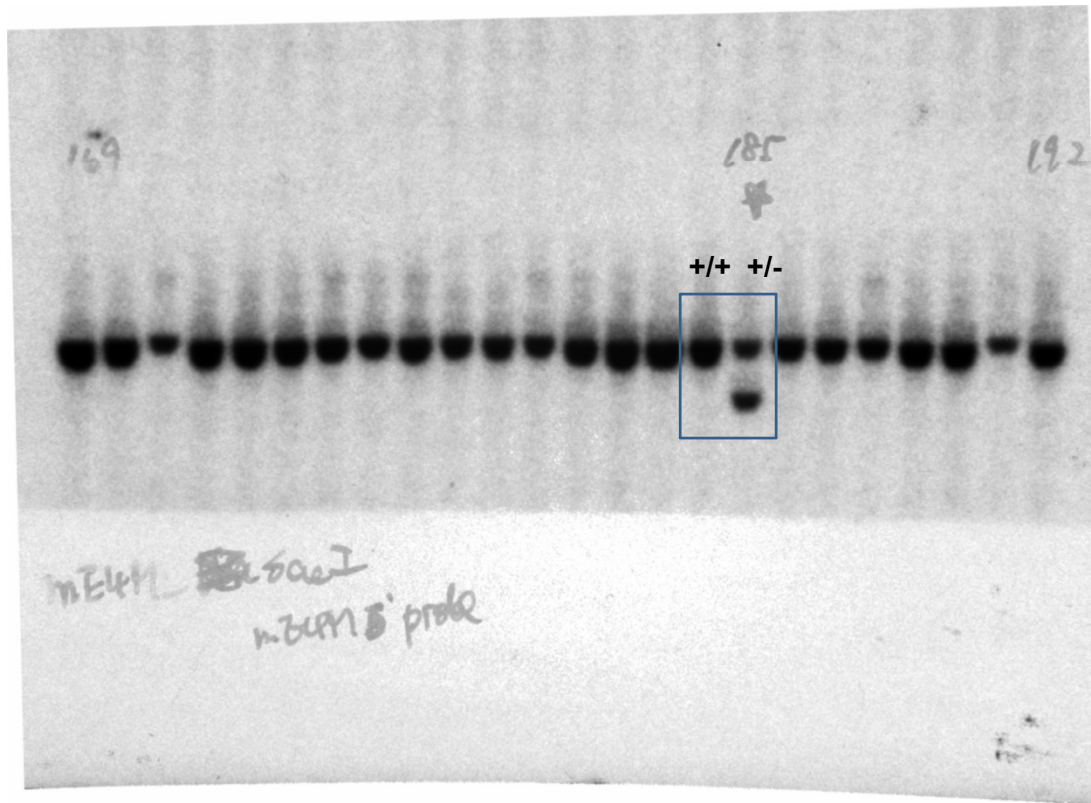


Figure S2C. mE4M (SacI) ES cell: W4.

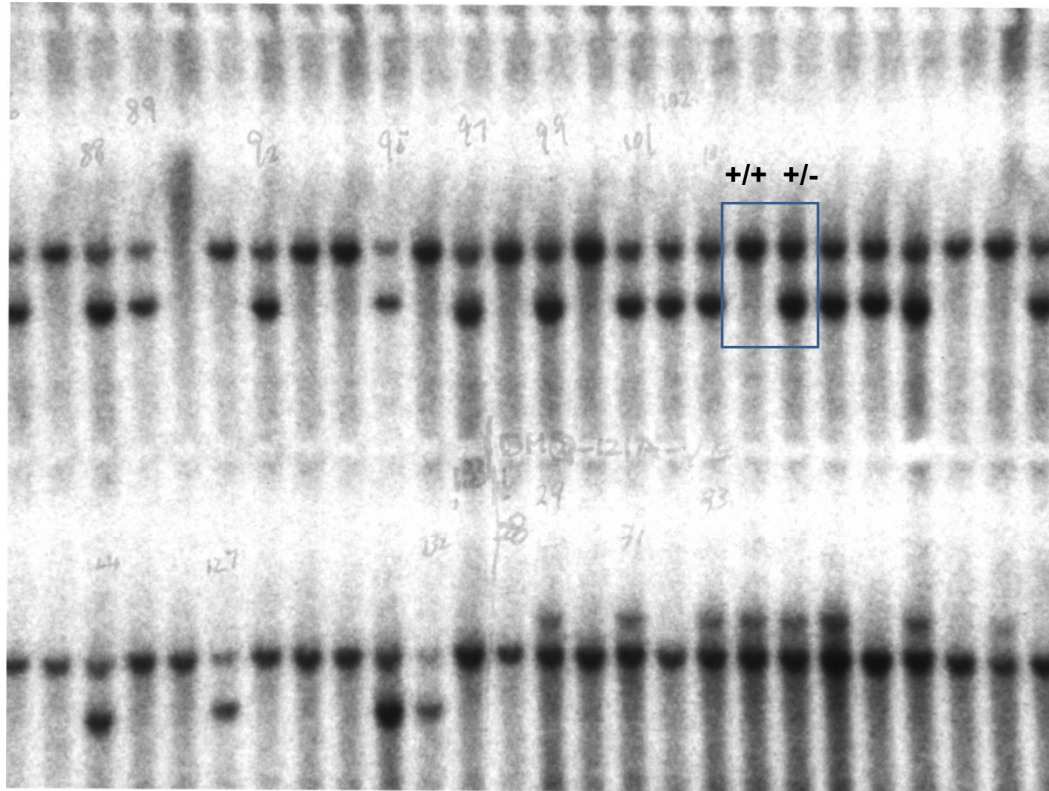


Figure S2C. mE4M Mouse tail.

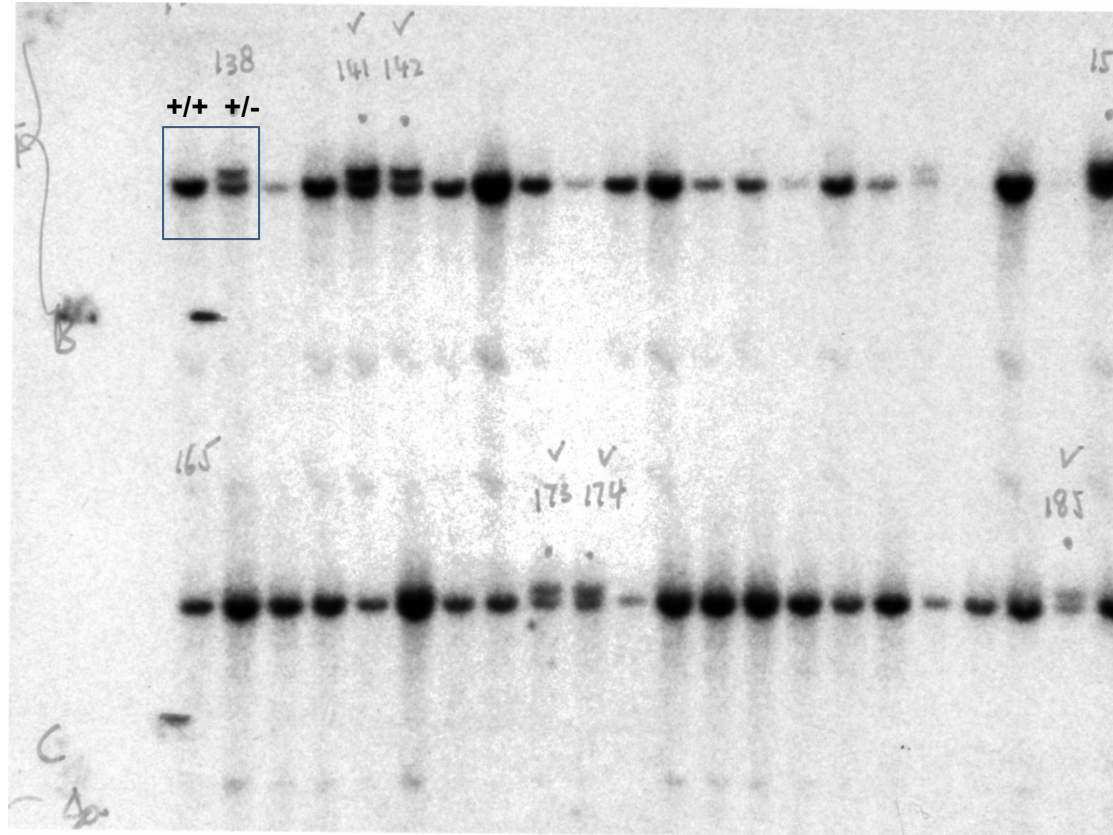


Figure S2C. mE7M (EcoRI) ES cell: W4.

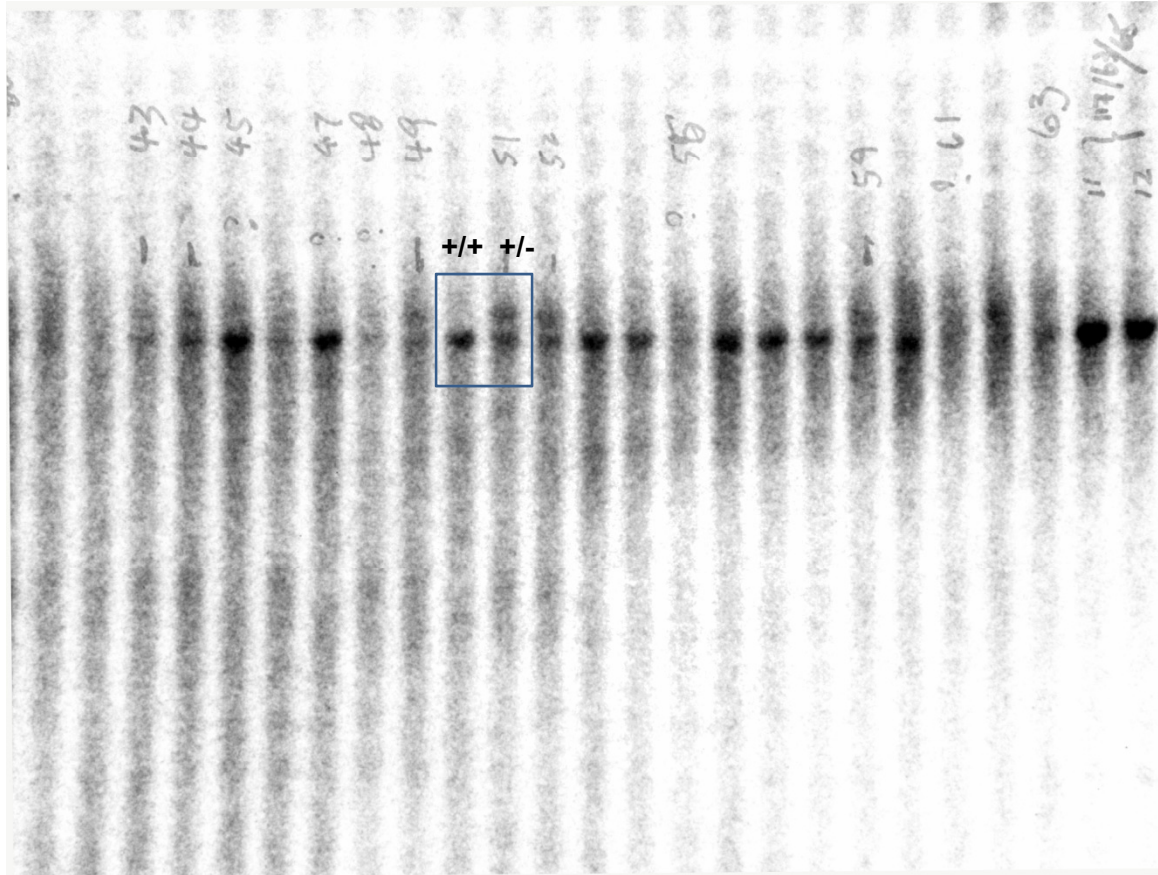


Figure S2C. mE7M Mouse tail.

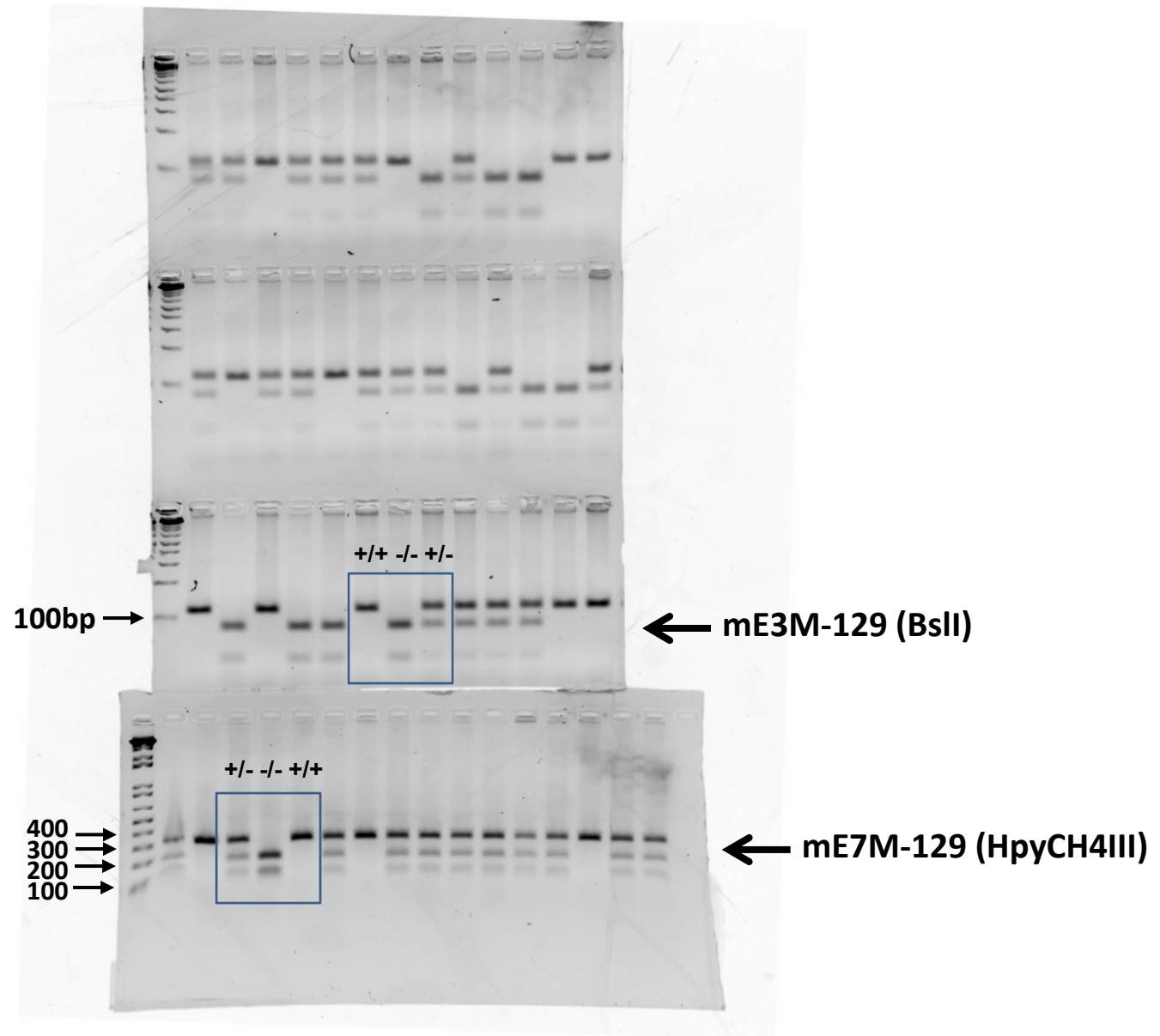


Figure S2D. mE3M-129 (BslI) and mE7M-129 (HpyCH4III).

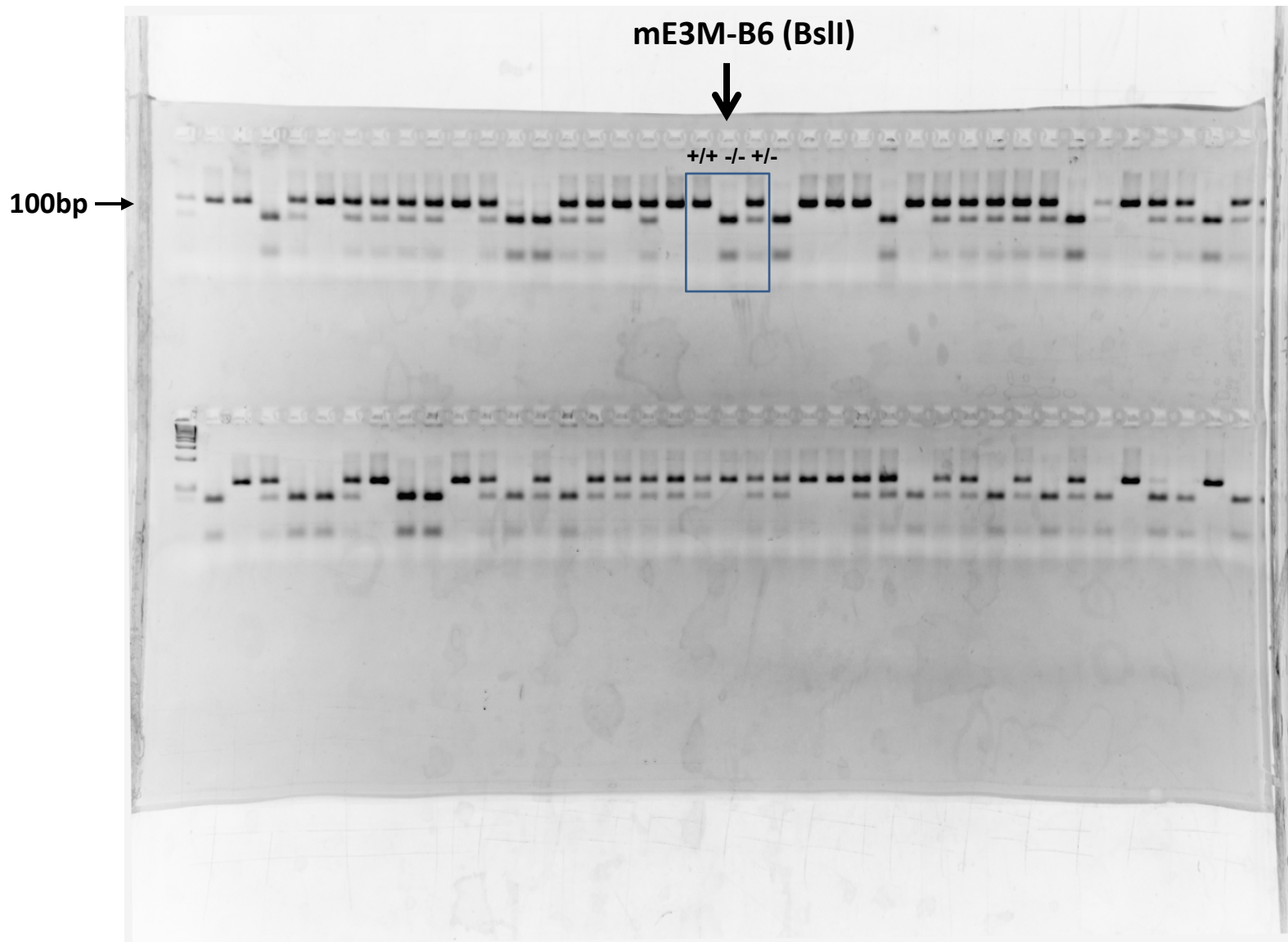


Figure S2D. mE3M-B6 (BslI).

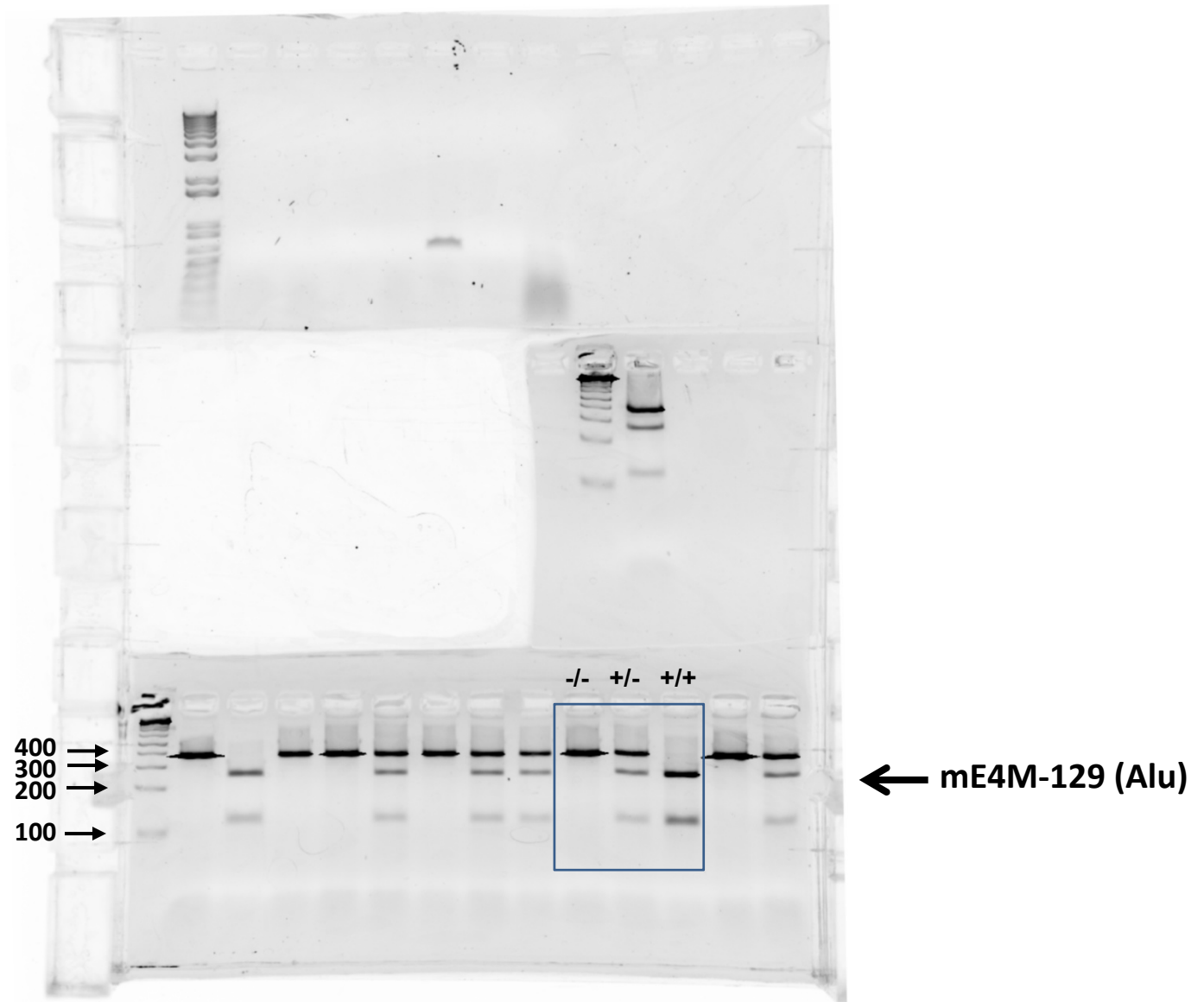


Figure S2D. mE4M-129 (Alu).

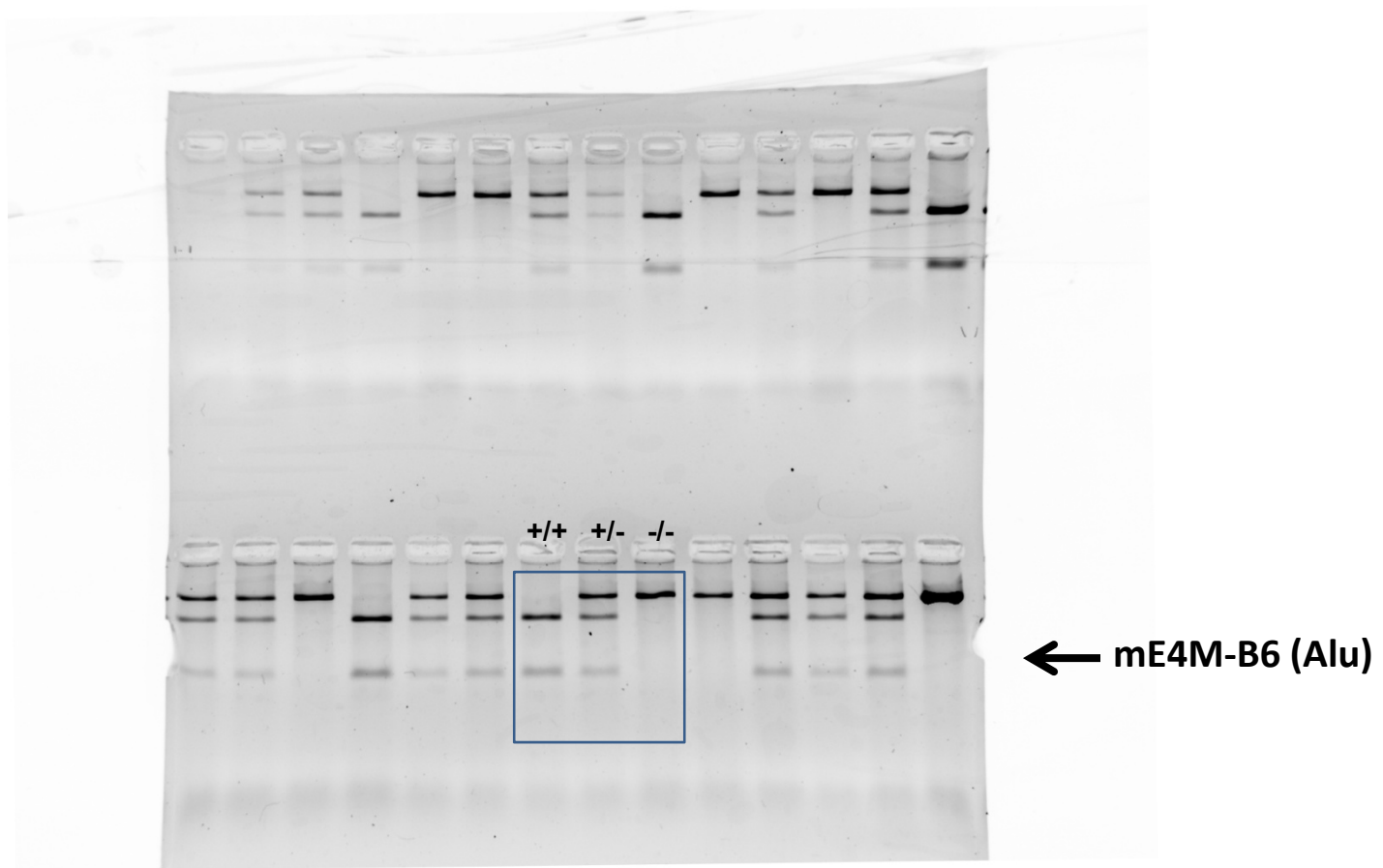


Figure S2D. mE4M-B6 (Alu).

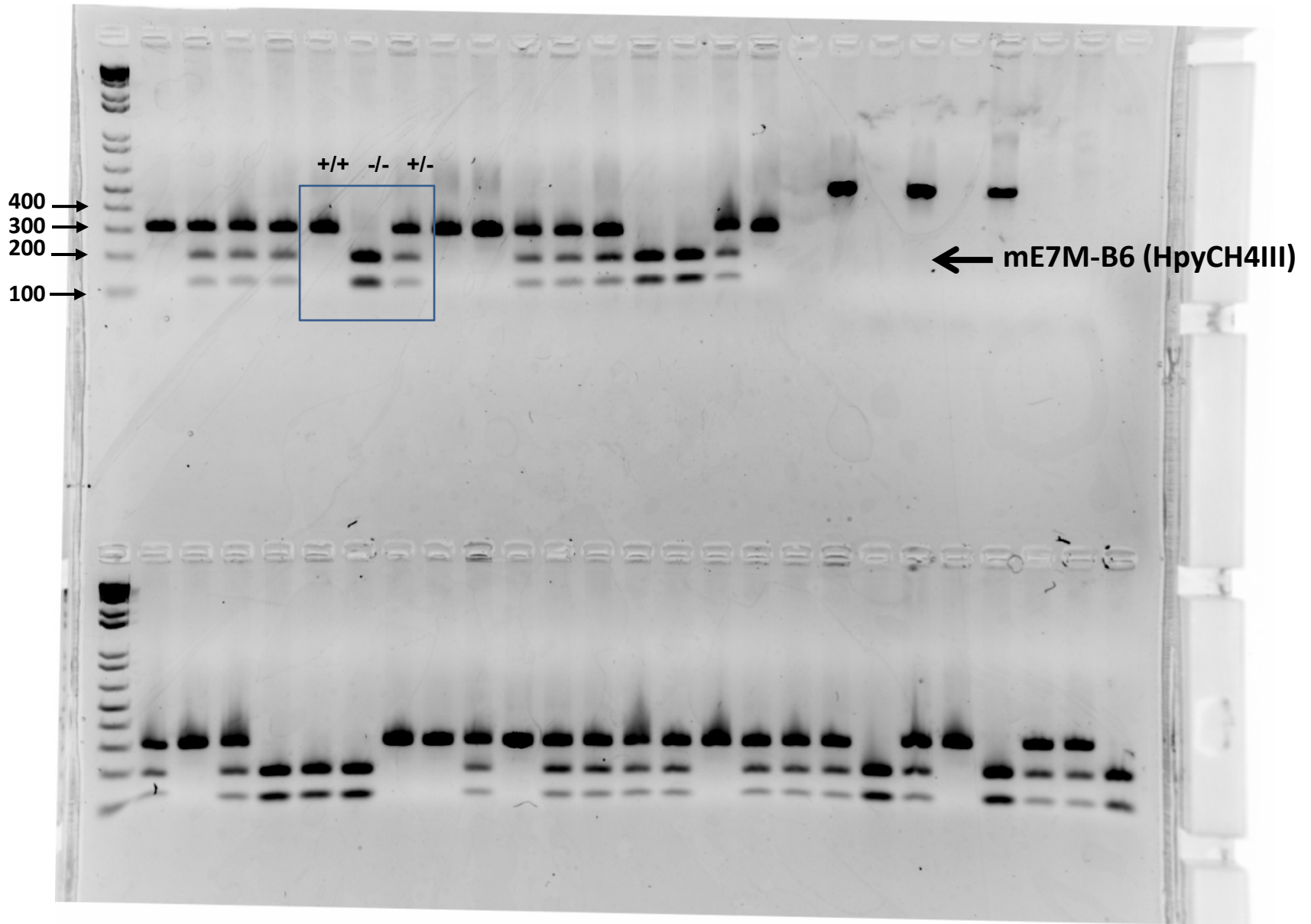


Figure S2D. mE7M-B6 (HpyCH4III).

1_mM1E3se.ab1

Sample name: 1-mM1E3se

Avg. intensity: G-1050, A-1120, T-1219, C-566

Page 1 of 9

Lane: 96 / 96

Mobility file: KB_3730_POP7_BDTv3.mob

Position: A12

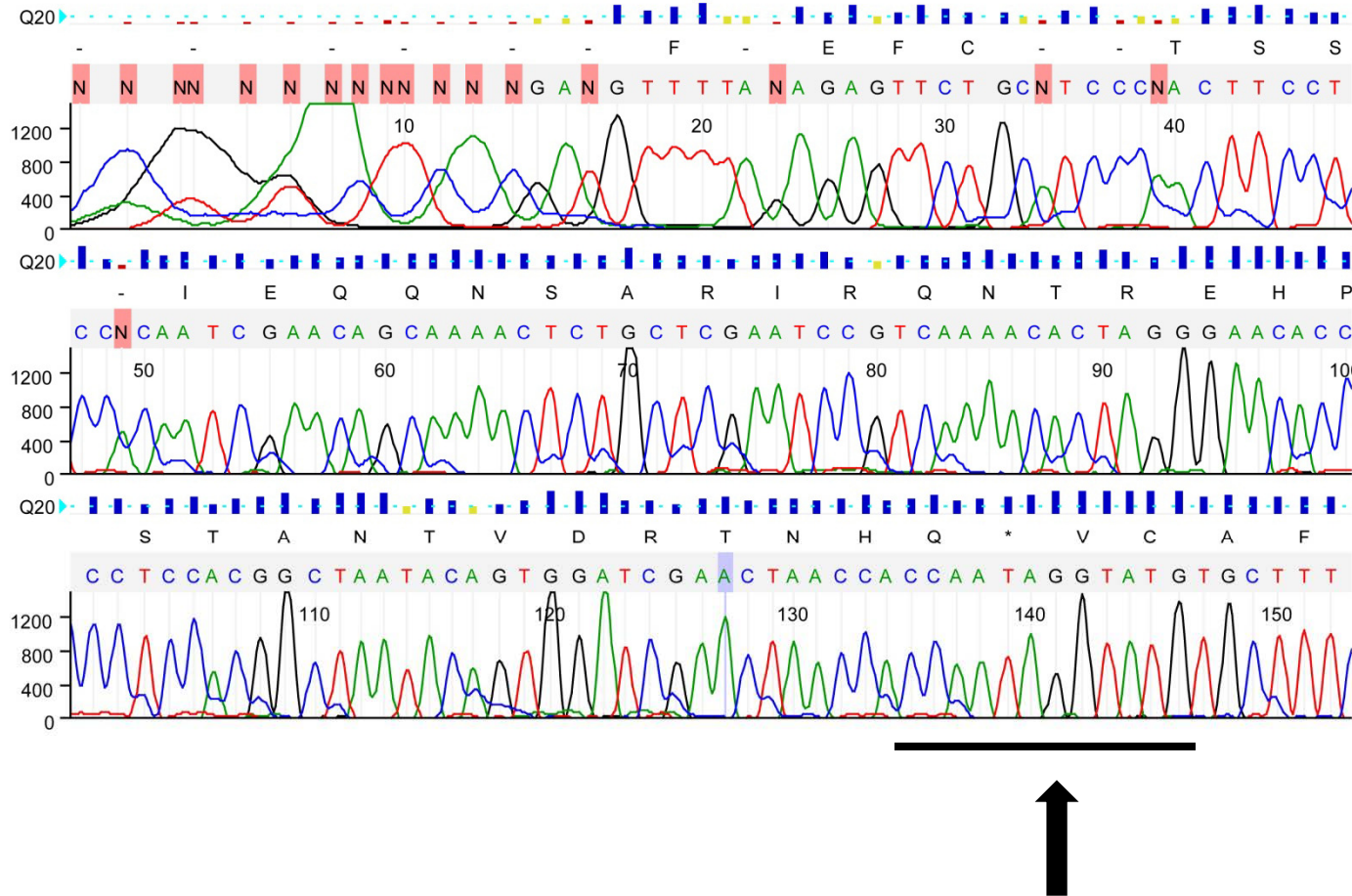


Figure S2E. mE3M-129 genomic DAN sequence.

2_mM1E3se.ab1

Sample name: 2-mM1E3se

Avg. intensity: G-323, A-342, T-393, C-186

Lane: 94 / 96

Mobility file: KB_3730_POP7_BDTv3.mob

Position: B12

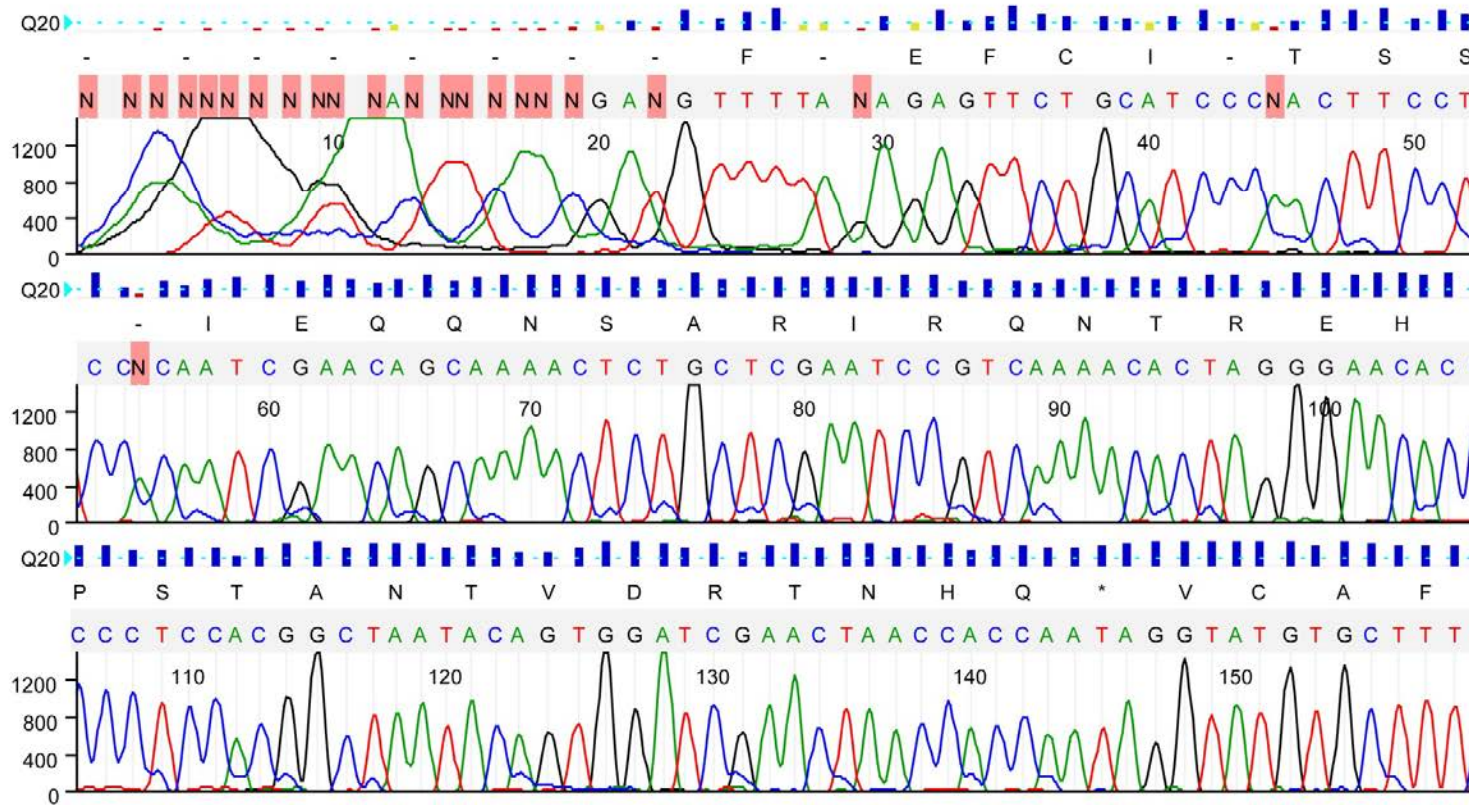


Figure S2E. mE3M-B6 genomic DAN sequence.

3_mE4Mpcrs.ab1

Sample name: 3-mE4Mpcrs
Lane: 92 / 96
Position: C12

Avg. intensity: G-288, A-242, T-365, C-209
Mobility file: KB_3730_POP7_BDTV3.mob

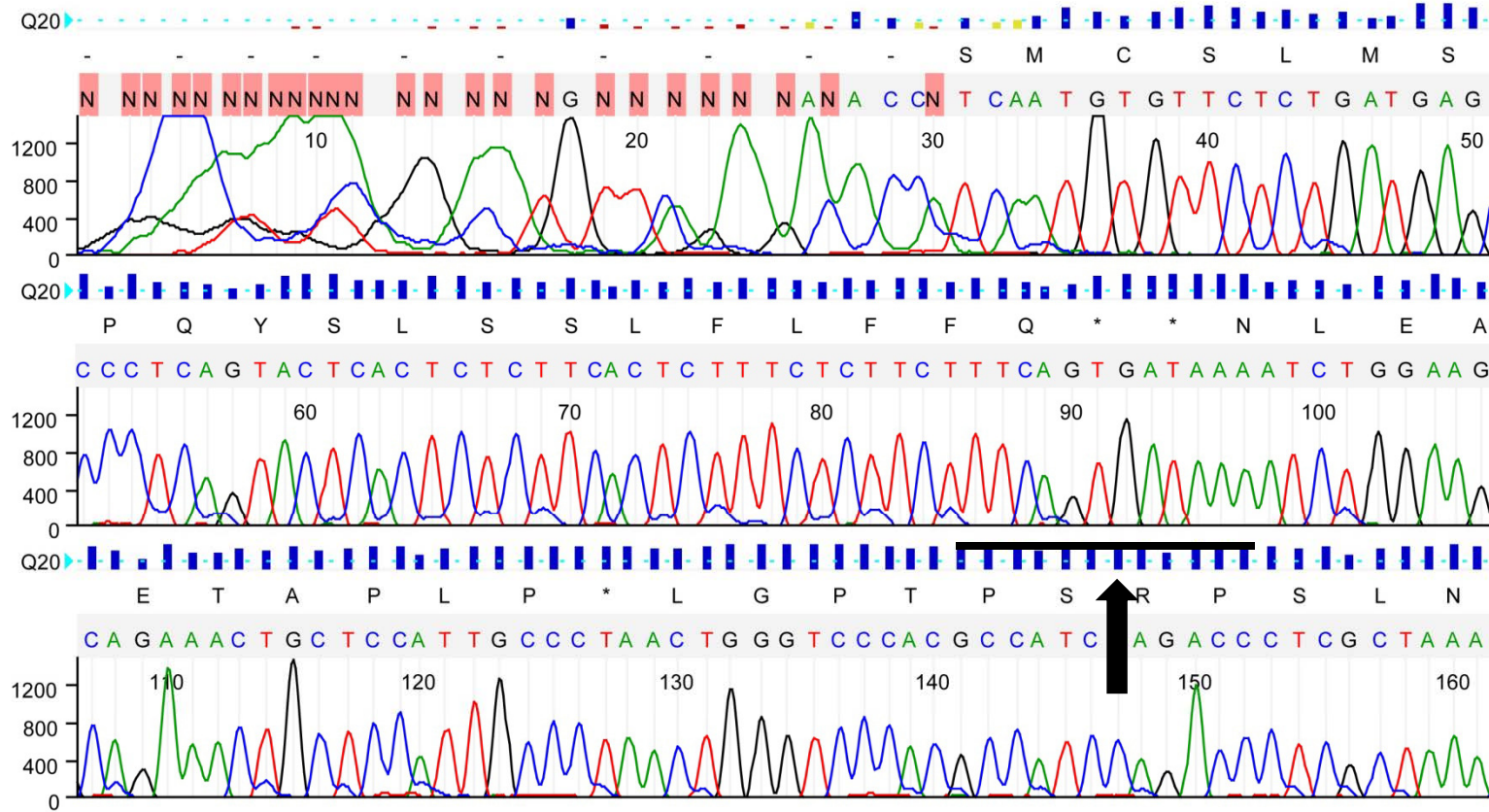


Figure S2E. mE4M-129 genomic DAN sequence.

5_mE7Mpcrs.ab1

Sample name: 5-mE7Mpcrs

Avg. intensity: G-336, A-215, T-244, C-177

Lane: 88 / 96

Mobility file: KB_3730_POP7_BDTv3.mob

Position: E12

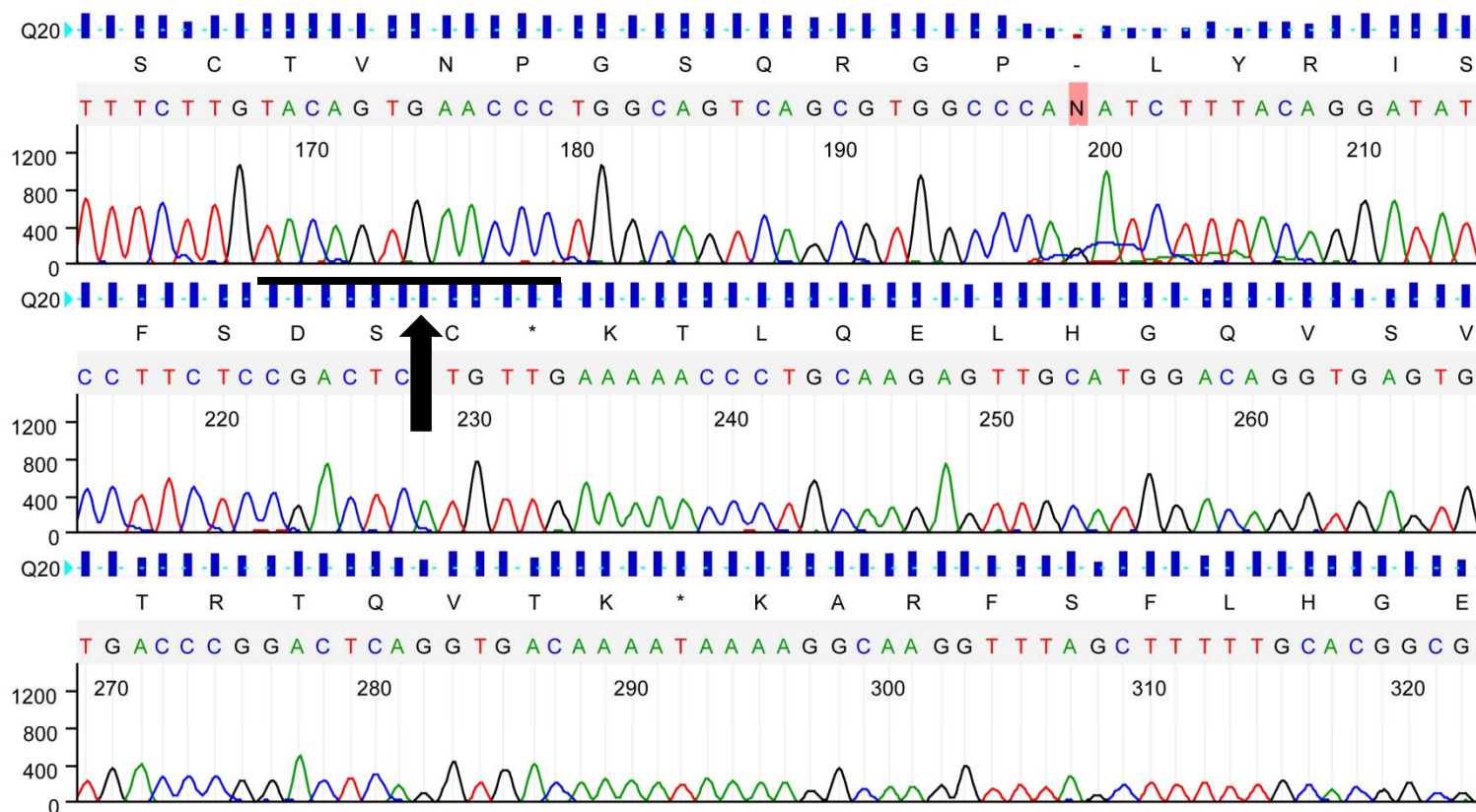


Figure S2E. mE7M-129 genomic DAN sequence.

6_me7Mpcrs.ab1

Sample name: 6-me7Mpcrs

Avg. intensity: G-721, A-493, T-700, C-429

Lane: 86 / 96

Mobility file: KB_3730_POP7_BDTv3.mob

Position: F12

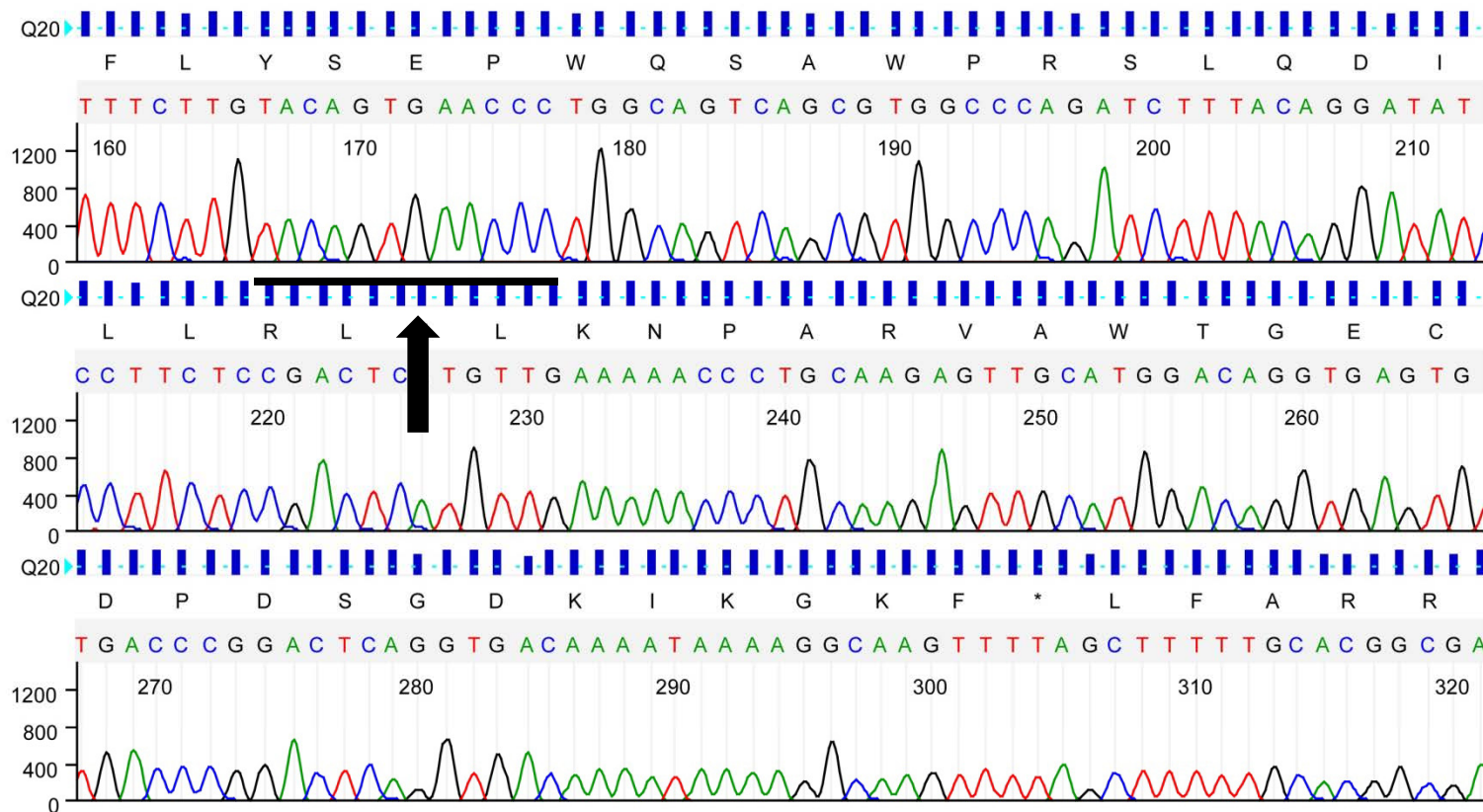


Figure S2E. mE7M-B6 genomic DAN sequence.

2_1271se.ab1

Sample name: 2-1271se

Avg. intensity: G-261, A-188, T-151, C-171

Lane: 4 / 96

Mobility file: KB_3730_POP7_BDTV3.mob

Position: G2

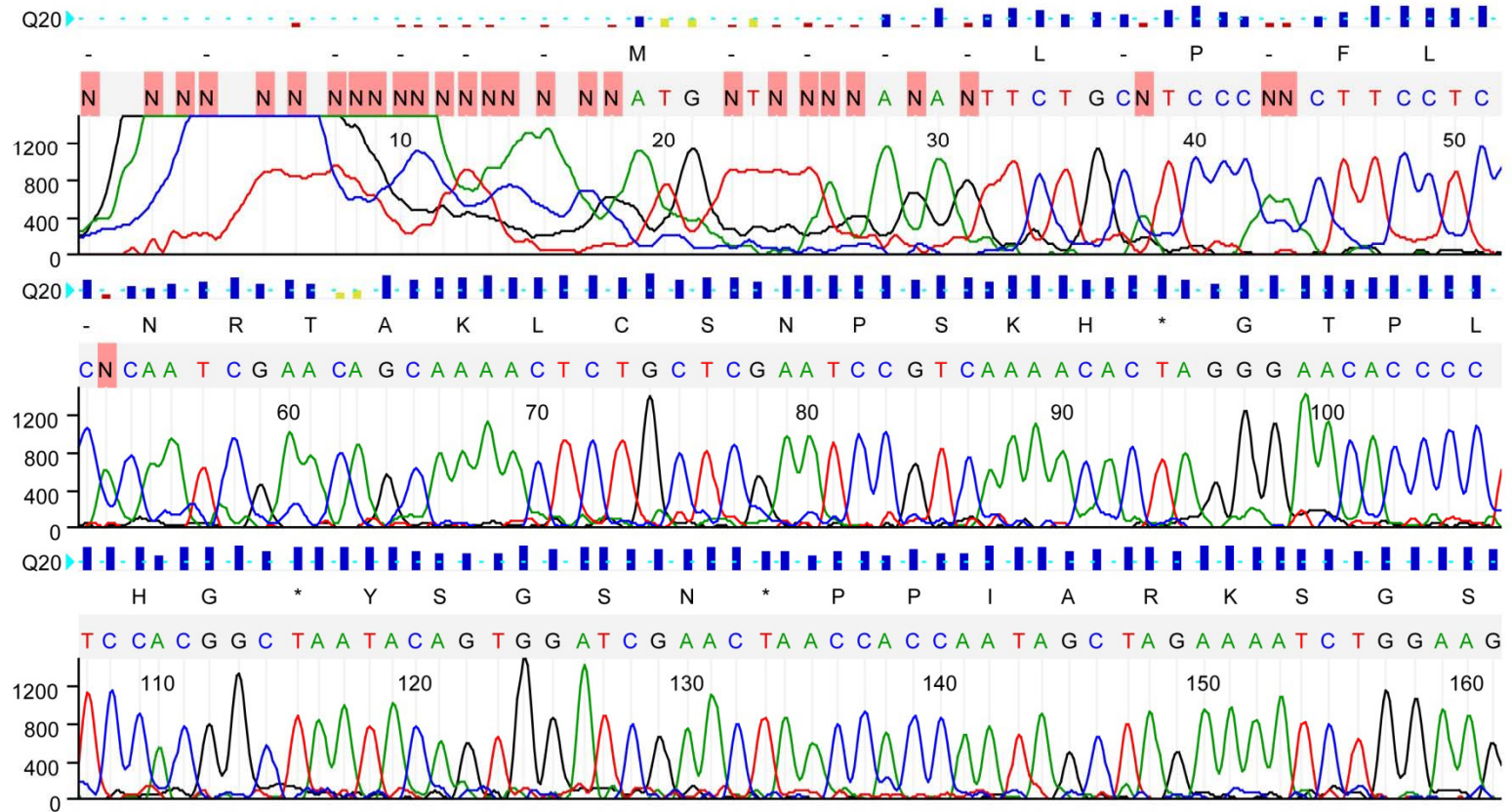


Figure S2F. mE3M-129 RT-PCR sequence.

4_1271se.ab1

Sample name: 4-1271se

Avg. intensity: G-502, A-372, T-301, C-361

Lane: 31 / 96

Mobility file: KB_3730_POP7_BDTv3.mob

Position: A3

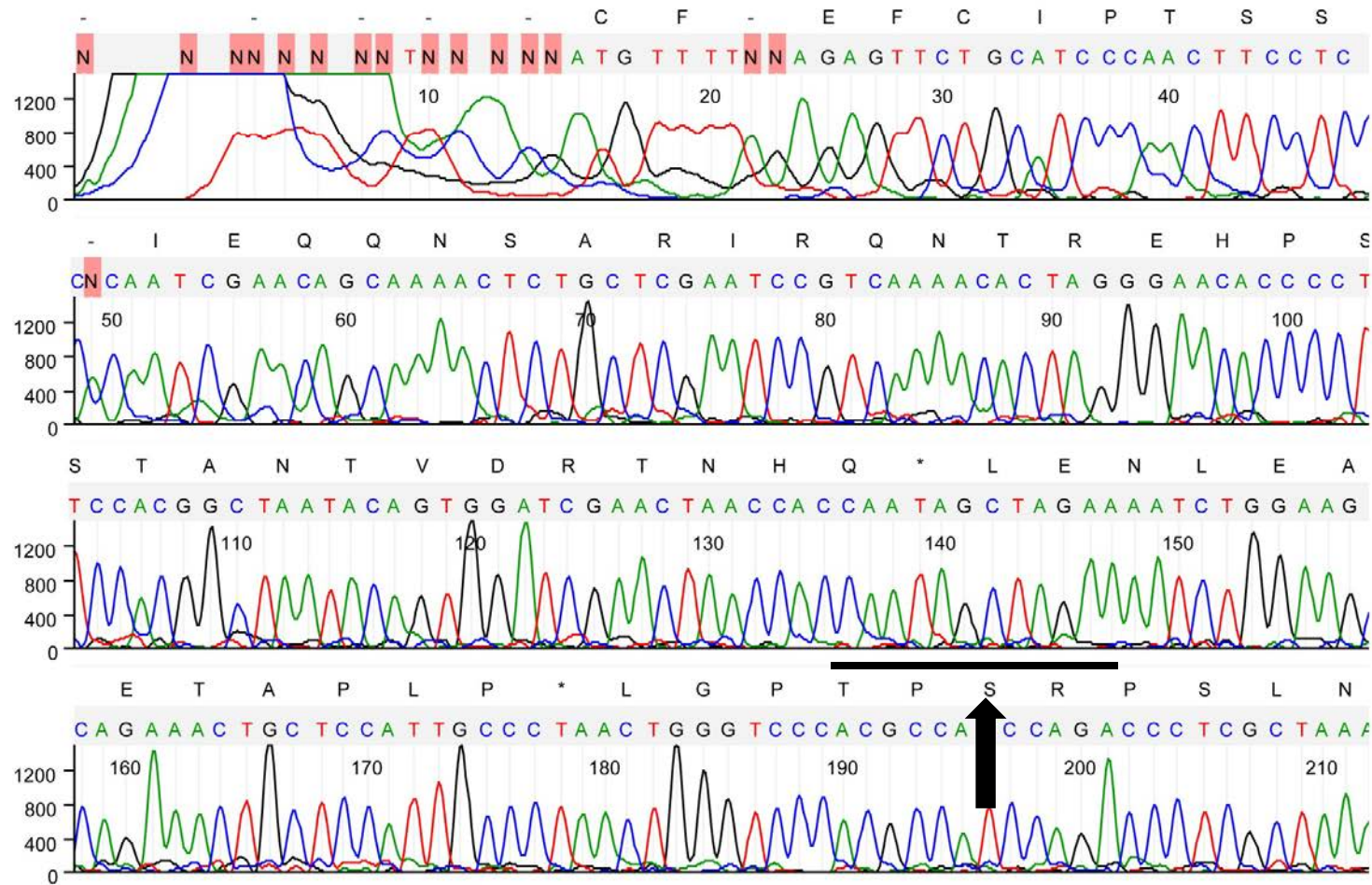


Figure S2F. mE3M-B6 RT-PCR sequence.

6_e34an.ab1

Sample name: 6-e34an
Lane: 27 / 96
Position: C3

Avg. intensity: G-1385, A-876, T-1163, C-757
Mobility file: KB_3730_POP7_BDTv3.mob

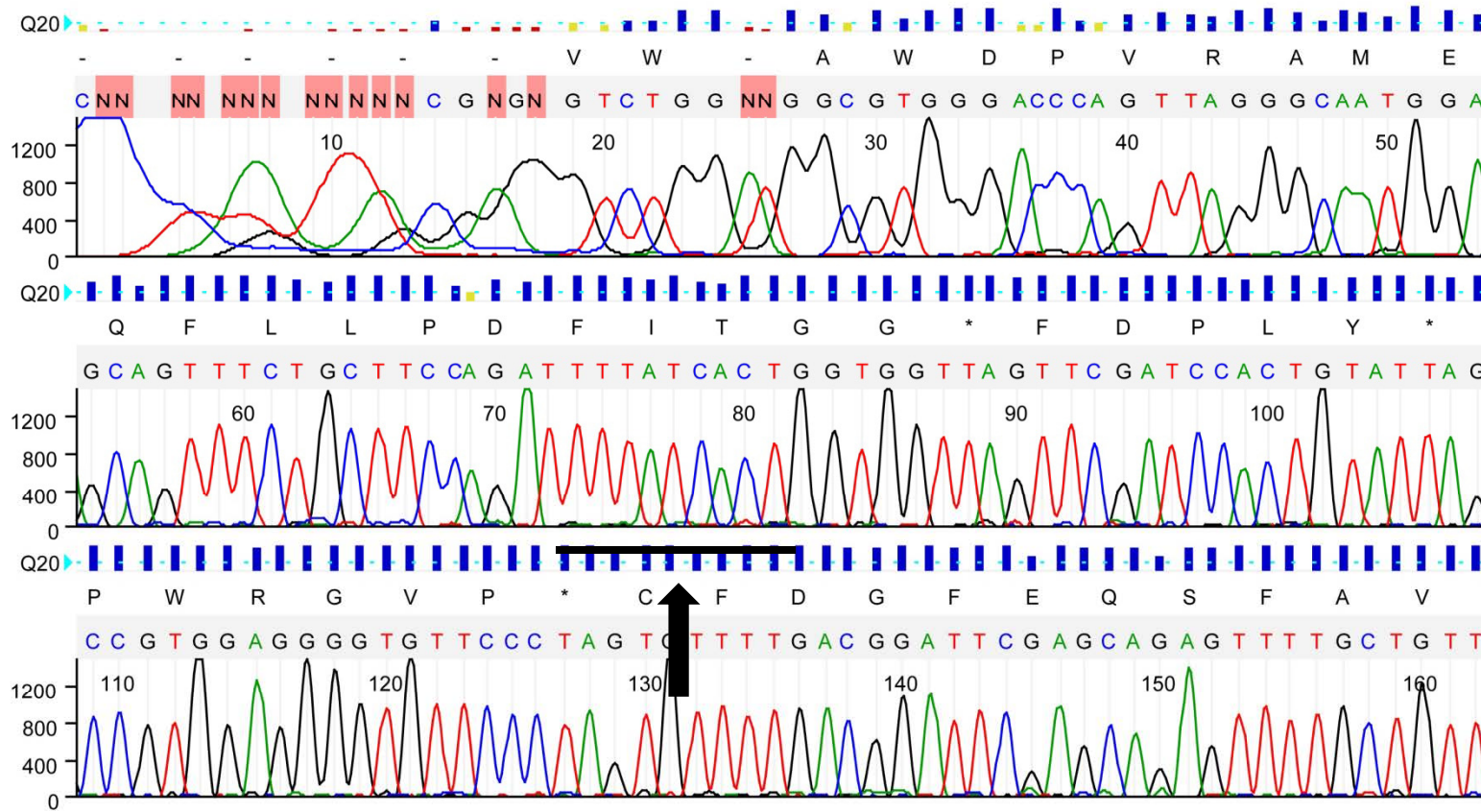


Figure S2F. mE4M-129 RT-PCR sequence.

8_e34an.ab1

Sample name: 8-e34an
Lane: 23 / 96
Position: E3

Avg. intensity: G-996, A-607, T-747, C-540
Mobility file: KB_3730_POP7_BDTv3.mob

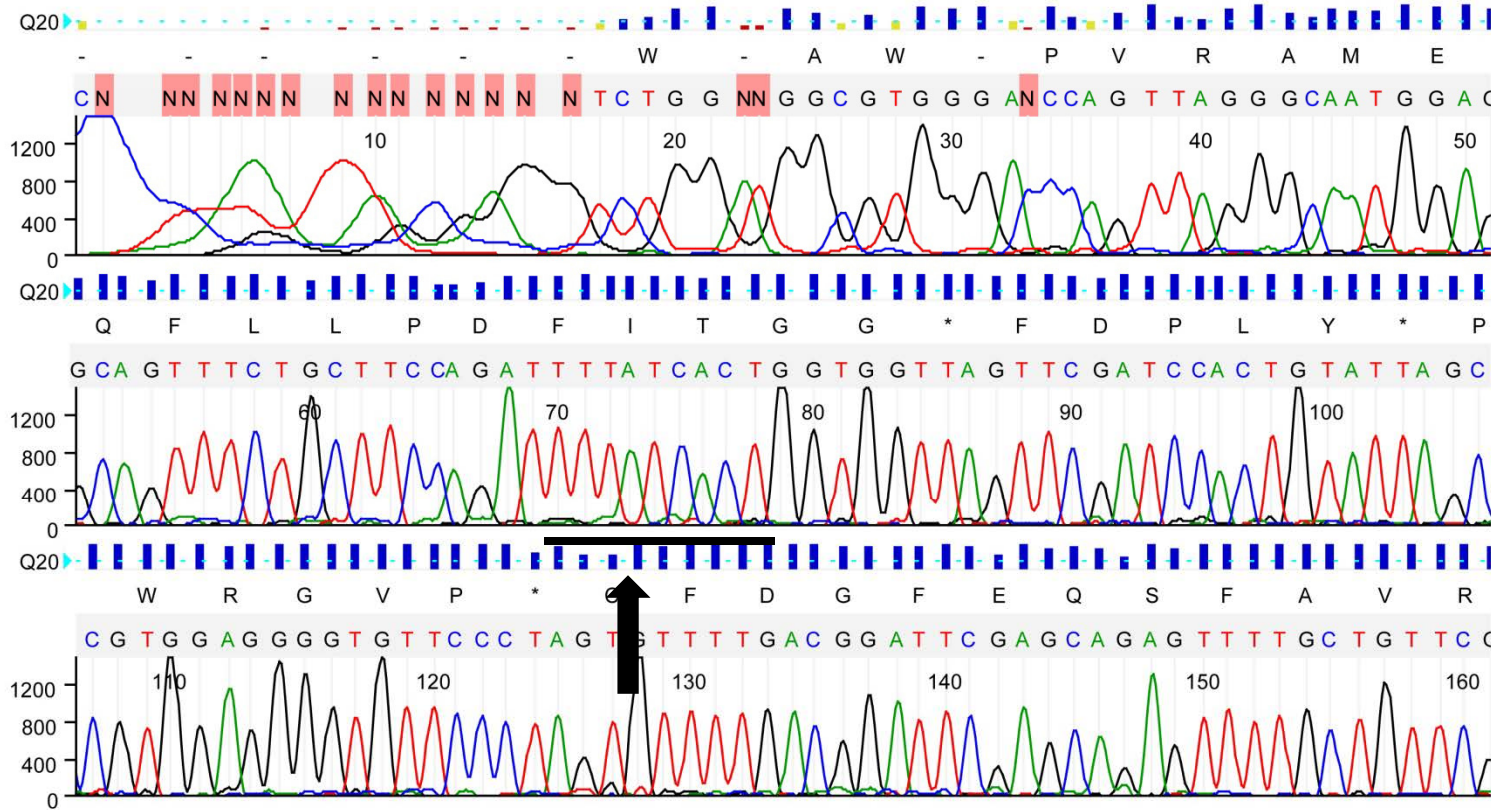


Figure S2F. mE4M-B6 RT-PCR sequence.

6b_89an.ab1

Sample name: 6b-89an

Avg. intensity: G-316, A-204, T-199, C-166

Lane: 12 / 96

Mobility file: KB_3730_POP7_BDTv3.mob

Position: C2

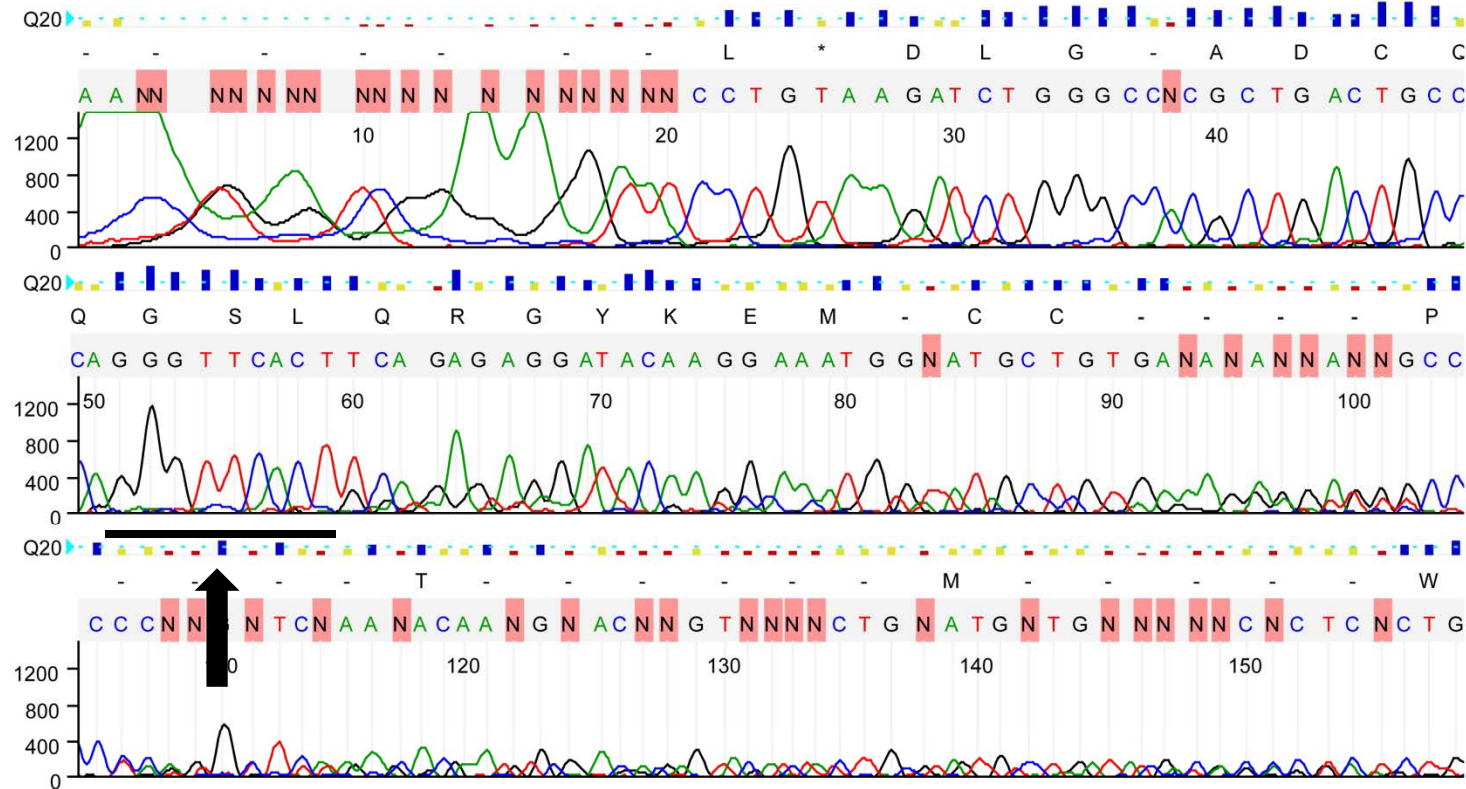


Figure S2F. mE7M-129 RT-PCR sequence.

8a_89an.ab1

Sample name: 8a-89an

Avg. intensity: G-482, A-298, T-315, C-221

Lane: 8 / 96

Mobility file: KB_3730_POP7_BDTv3.mob

Position: E2

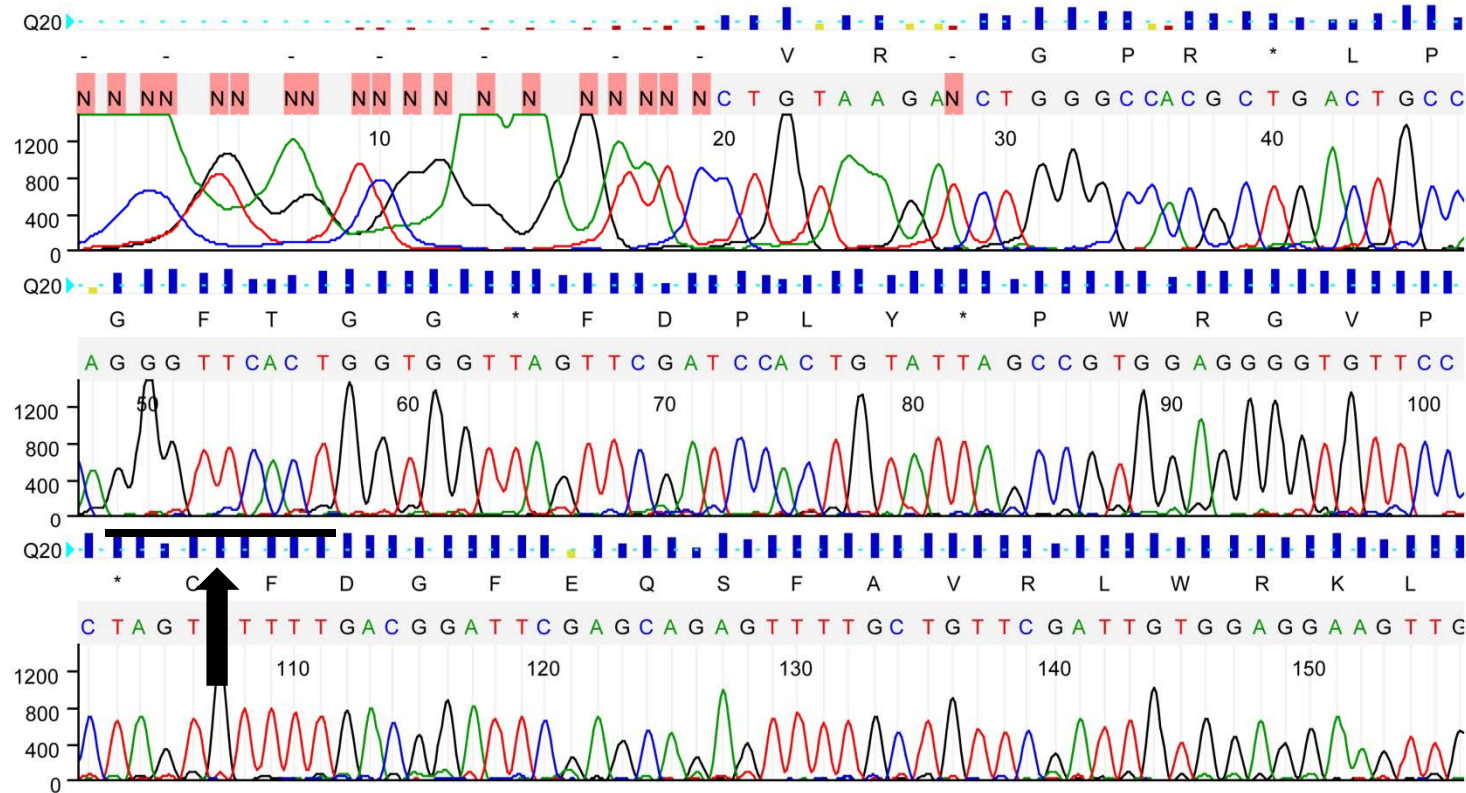


Figure S2F. mE7M-B6 RT-PCR sequence.

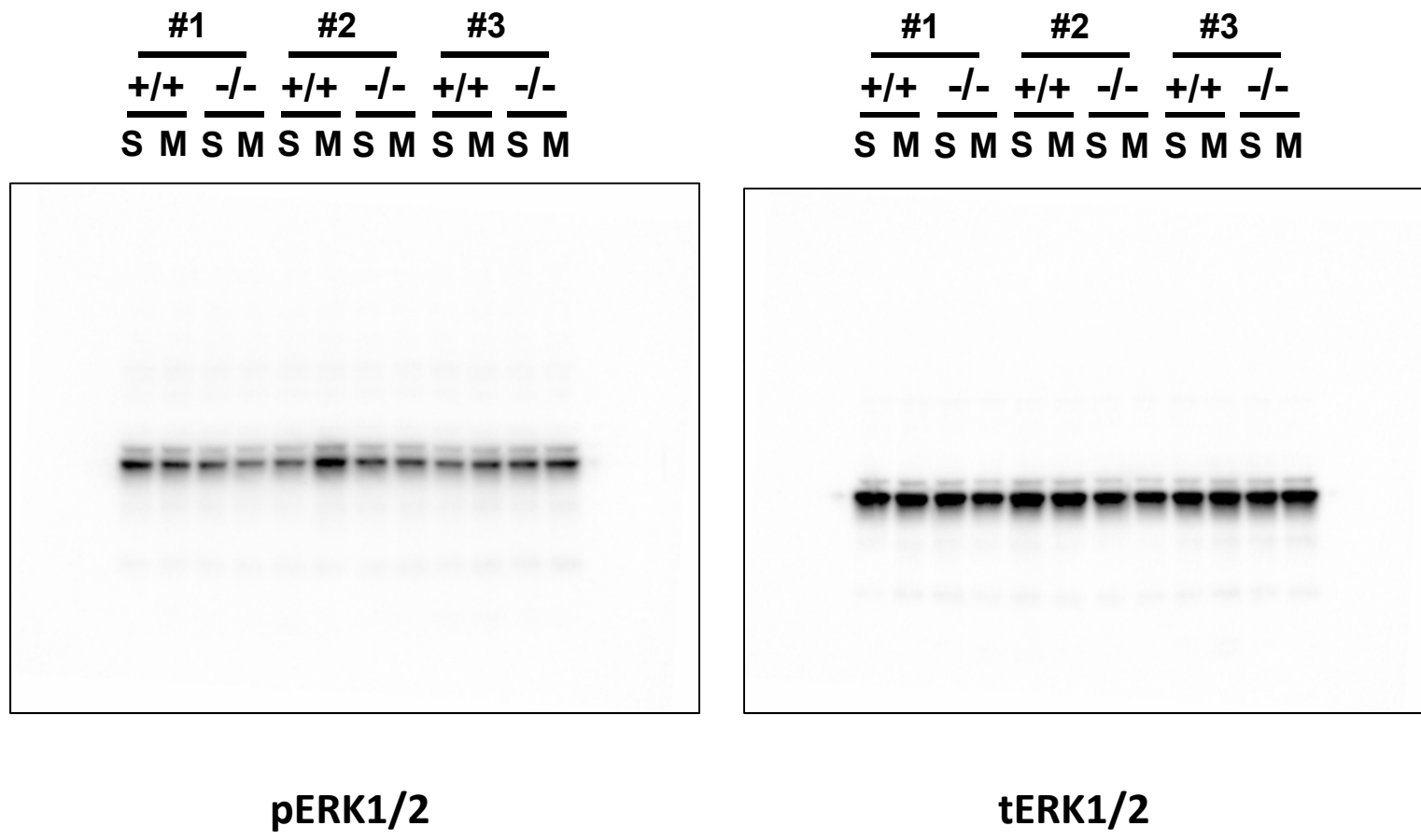


Figure S9. Western blot of morphine-induced ERK1/2 activation in the striatum.

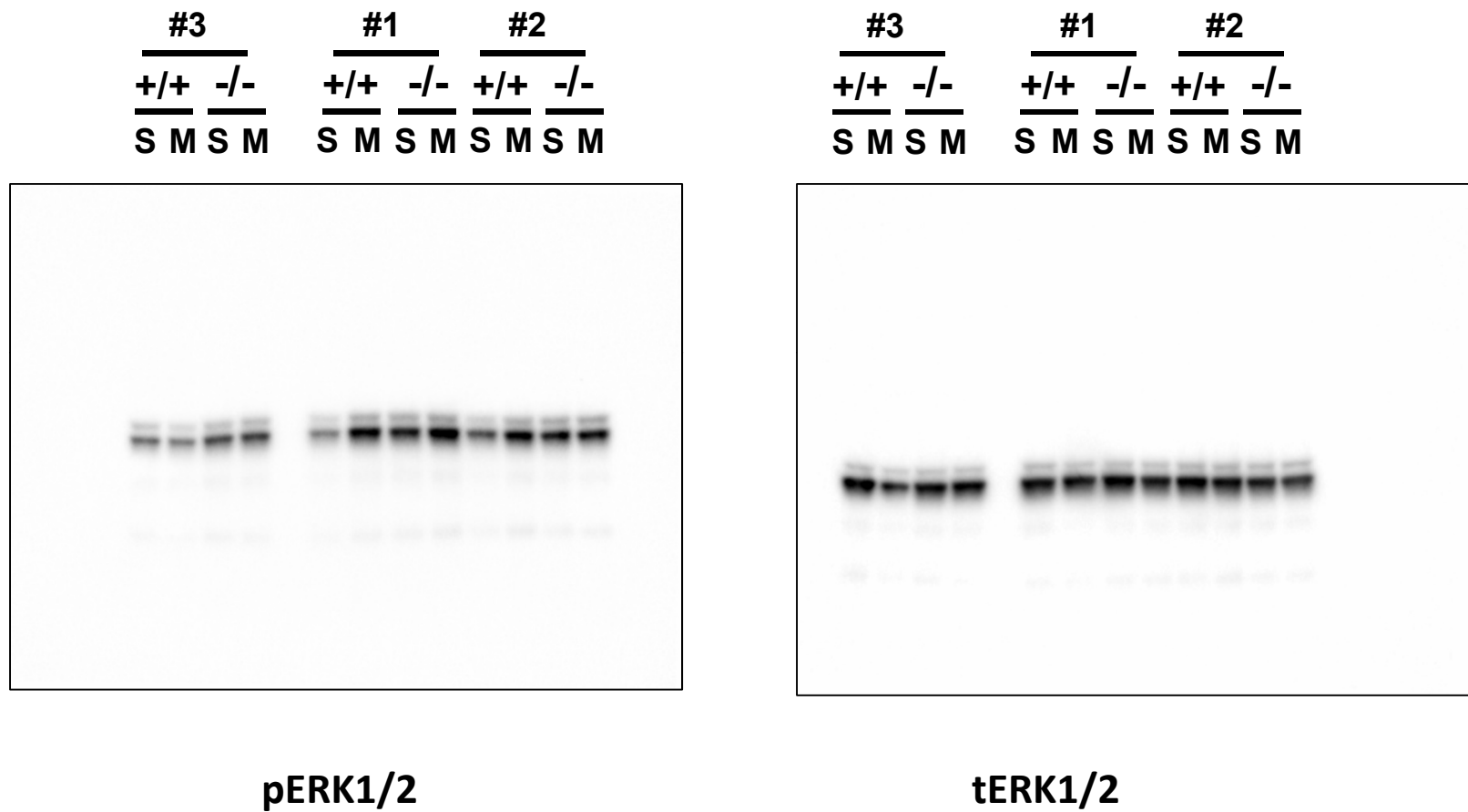


Figure S9. Western blot of morphine-induced ERK1/2 activation in the nucleus accumbens.

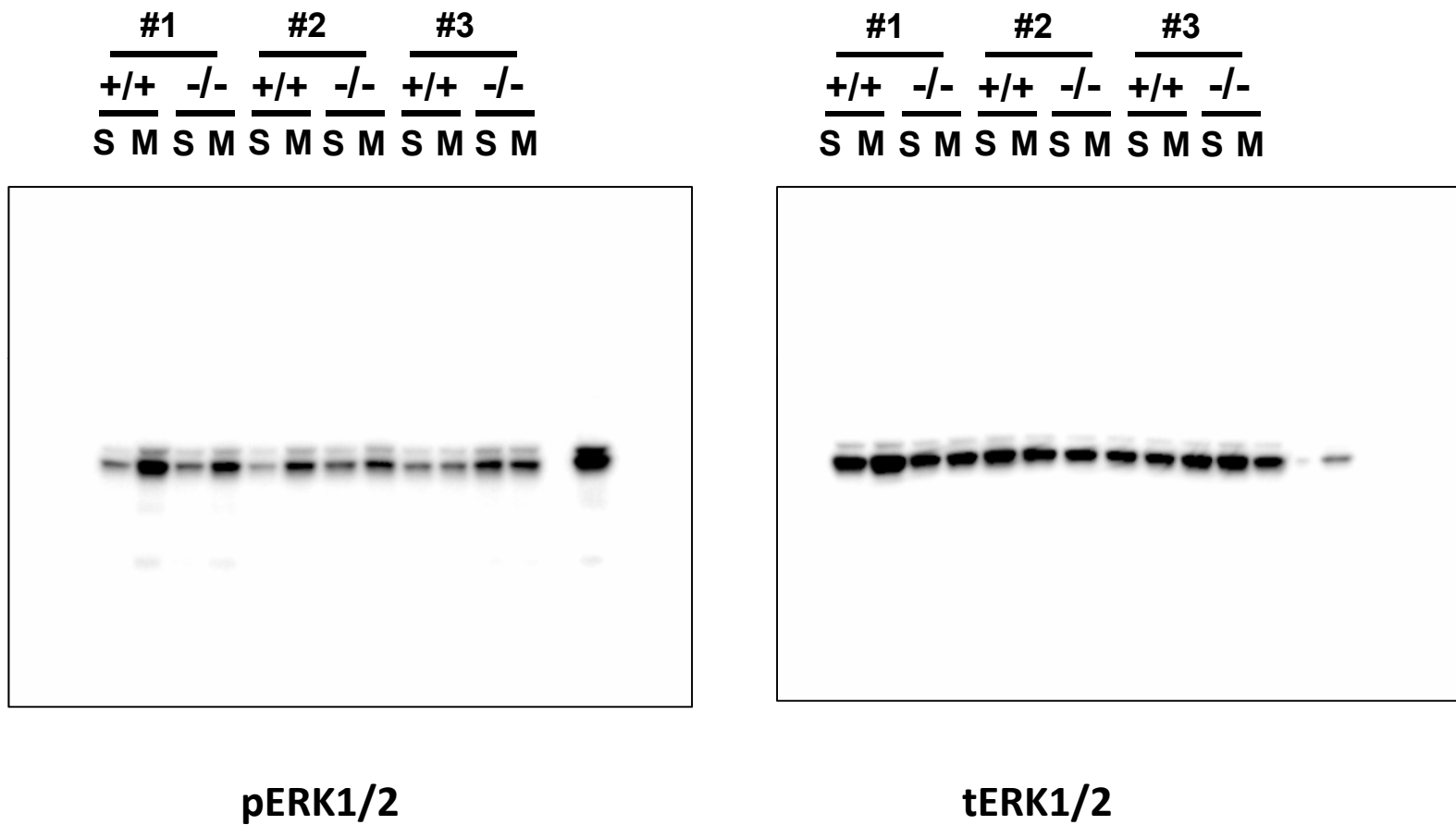
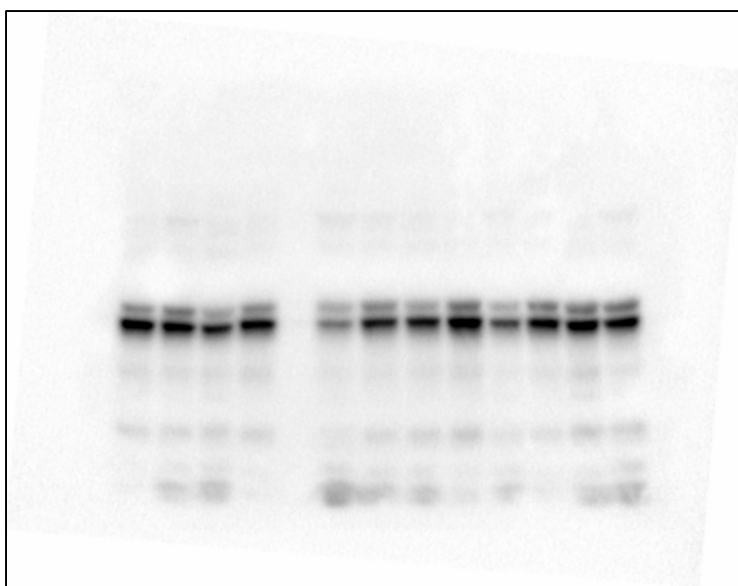


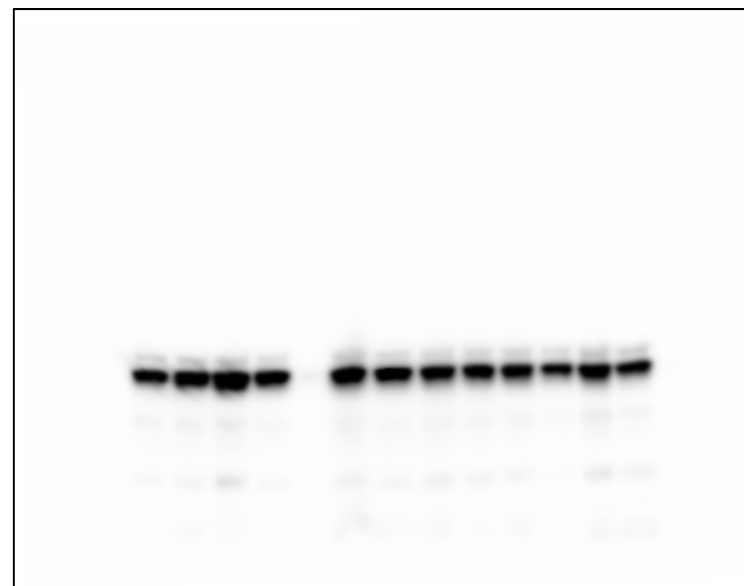
Figure S9. Western blot of morphine-induced ERK1/2 activation in the thalamus.

<u>#3</u>		<u>#1</u>		<u>#2</u>	
<u>+/+</u>	<u>-/-</u>	<u>+/+</u>	<u>-/-</u>	<u>+/+</u>	<u>-/-</u>
S	M	S	M	S	M

<u>#3</u>		<u>#1</u>		<u>#2</u>	
<u>+/+</u>	<u>-/-</u>	<u>+/+</u>	<u>-/-</u>	<u>+/+</u>	<u>-/-</u>
S	M	S	M	S	M



pERK1/2



tERK1/2

Figure S9. Western blot of morphine-induced ERK1/2 activation in the hypothalamus.

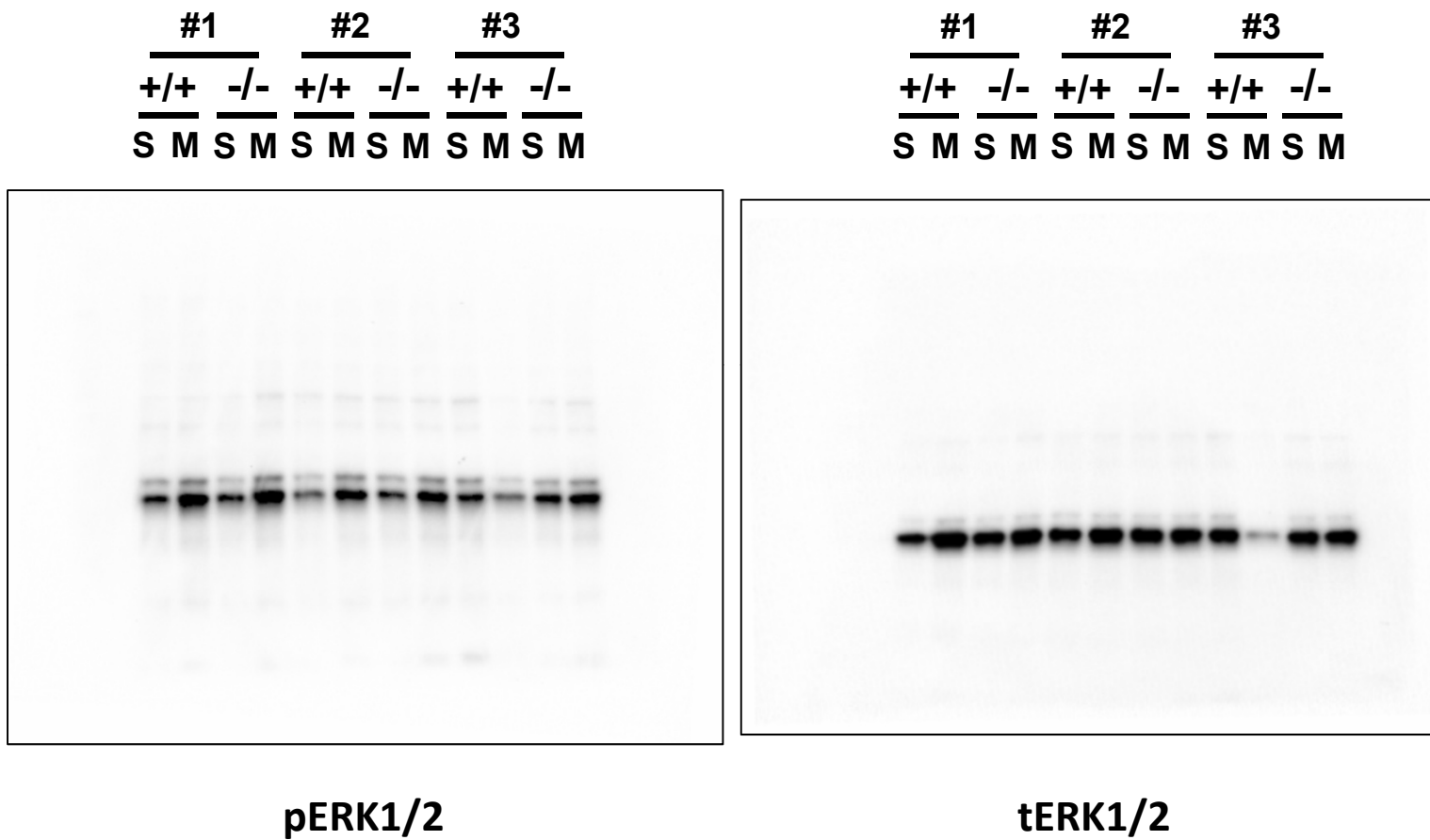
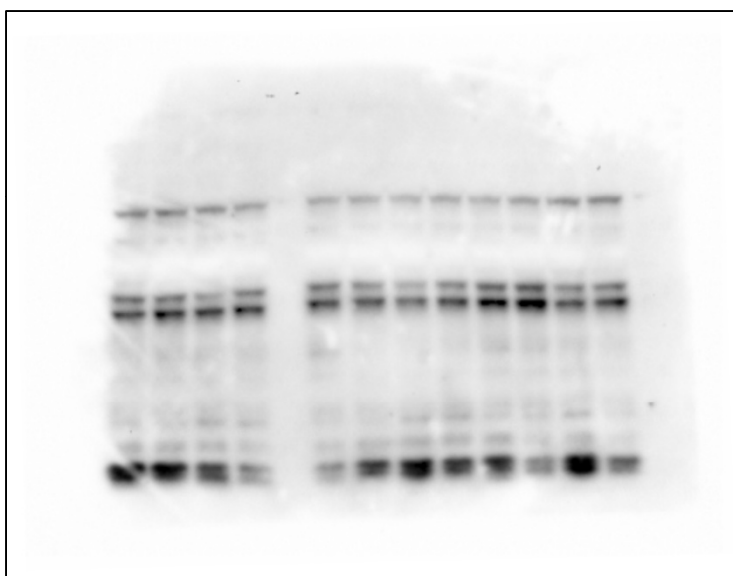


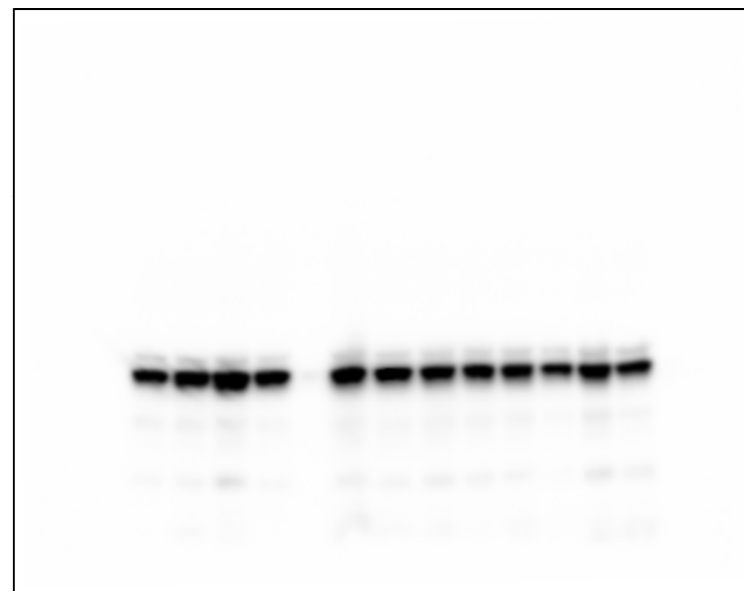
Figure S9. Western blot of morphine-induced ERK1/2 activation in the PAG.

<u>#3</u>		<u>#1</u>		<u>#2</u>	
+/+	-/-	+/+	-/-	+/+	-/-
S	M	S	M	S	M

<u>#3</u>		<u>#1</u>		<u>#2</u>	
+/+	-/-	+/+	-/-	+/+	-/-
S	M	S	M	S	M



pERK1/2



tERK1/2

Figure S9. Western blot of morphine-induced ERK1/2 activation in the brainstem.